Quantum dots and artificial atoms

John H. Jefferson[1] and Wolfgang Häusler[2]

[1] *DERA, Electronics Sector, St. Andrews Road, Malvern,*

Worcs. WR14

3PS, United Kingdom

[2] *I. Institut für Theoretische Physik, Jungiusstr. 9, 20355 Hamburg,*

Federal Republic of Germany

(February 1, 2008)

The electronic properties of nanoscale quantum dots are reviewed. The similarities and differences between these 'artificial atoms' and real atoms are discussed and, in particular, the effect of electron correlations is examined. It is shown that for (semiconductor) quantum dots, with only a few electrons, electron correlations can give rise to important new physics which is absent in their true atomic counterparts.

I. INTRODUCTION

In 1985 R.P.Feynman made the following prophetic statement. "*It seems to me that the laws of physics present no barrier to reducing the size of computers until bits are the size of atoms and quantum behaviour holds sway* " [1]. Well, here we are only a decade later and technological advances in microfabrication have enabled us to not only manipulate individual atoms but even single electrons. It is the manipulation of single-electrons, and the properties of a few interacting electrons confined on small islands of semiconducting material, called 'quantum dots', that we shall be concerned with here. Such quantum dots typically consist of a few hundred to a few million atoms are thus still some way from being the single atoms to which Feynman referred. Nevertheless, these quantum dot islands can behave in many ways like single atoms as pointed out by Kastner, who coined the term 'artificial atom' [2]. Certainly they can exhibit many of the quantum effects associated with their true atomic counterparts, where likewise few electrons are held together by the nuclear potential. However, these structures exhibit new physics which, whilst being quantum in origin, have no analogue in real atoms and influences their electrical properties. These effects, which we will describe below, are due to the interactions between the electrons. It turns out that *correlations* dominate the physics in many cases and render the independent-electron approximation useless, leading to even qualitatively incorrect results [3]. This should be compared with real atoms for which Hartree-Fock is an excellent approximation, providing at least the correct qualitative behaviour of atoms and a means for obtaining solutions of arbitrary accuracy in a controlled way by configuration mixing and perturbation theory. The origin of this different behaviour for artificial atoms with a small number of electrons is the nature of the confining potential which, being usually harmonic, is much more shallow than the $1/r$ potential of real atoms. This results in a lower electron density (larger mean separation between electrons) than is the case for atoms and the electron configurations can approach the classical (Wigner) limit in which the electrons are in fixed positions which minimise the electrostatic energy.

---

[02] Present address : Theoretical Physics Institute, 116 Church Str. SE Minneapolis MN 55455, U. S. A.

II. EXPERIMENTAL REALISATION

Single electron effects can be observed in the electrical transport properties of small conducting particles that are weakly coupled to their environment [4,5]. A simple example is a small (nanoscale) metallic grain surrounded by a thin insulating layer. Indeed such metallic 'dots' can be fabricated in a controlled way these days, for example gold particles encapsulated by organic molecules and placed on a gold surface [6]. Electrons can be made to tunnel into the dot and out through the substrate to produce a current using a fine probe such as an STM tip. When this is done, a finite voltage is required at low temperatures before any current is produced and the $I - V$ curve is antisymmetric about $V = 0$, as shown in Fig. 1. This finite turn-on voltage is referred to as the 'Coulomb gap' and occurs because of the very small capacitance of the island, as we explain in the next section. An even more spectacular effect is observed when a third (gate) electrode is introduced, as we describe below. A schematic diagram of one such structure, similar to that fabricated by Meirav *et al* [7], is shown in Fig. 2. It consists of a heterojunction between two semiconductors (such as GaAs and AlAs), a top and bottom gate (the top gate being patterned) and source and drain contacts. The wider gap semiconductor is doped with donors and the carriers migrate to the narrower gap semiconductor where they form a thin sheet of charge at the heterojunction interface, *i.e.* a quasi two-dimensional electron sheet (2DES). When the top gate is biased negatively, the electrons beneath it in the 2DES are repelled and, without the four 'stubs' on the gate, this would give rise to a thin filament of charge, converting the 2DES into a quasi one-dimensional wire. The purpose of the stubs is to give rise to barrier for electrons, which defines a small potential well, as shown in the electron potential energy diagram of Fig. 3. (This is for a plane close to the heterojunction interface where the charge density would be a maximum for the 2DES in the absence of the top gate.) The Fermi energy of the electrons near the heterojunction interface can be adjusted by changing the voltage on one or both gates. At low temperatures there is little or no current through the device when a small source-drain voltage is applied *except* in the region of certain gate voltages when a current flows. This behaviour is shown in the $I - V_G$ curve of Fig. 4. The current switches on and off as the gate voltage is increased. This behaviour can be explained roughly as follows (a more precise explanation will be given in the next section). The gate voltages may be adjusted such that the Fermi energy lies below the bottom of the quantum well but still above the quasi 1D 'leads' at either side of the well as shown in Fig. 5a, where the shaded region represents the quasi 1D Fermi sea. The forbidden gap region below the well is too wide to permit tunnelling in one jump from one lead to the other and hence at low temperature there is negligible current. If the gate voltage is adjusted so that the quantum well is lowered in energy (by making the bottom gate voltage more positive) then eventually the Fermi energy will be above the bottom of the well and a current will flow with electrons tunnelling into and out of the dot (Fig. 5b). This is rather like what happens in a field effect transistor (FET), which is 'switched on' by applying a gate voltage. However, unlike the FET, the device may be switched off by further increasing the gate voltage. This is because there are no empty states in the leads available for the electron to leave the dot when the well is lowered in energy. Furthermore, a second electron may also not enter the dot because of the large energy associated with the Coulomb repulsion between two electrons (or, equivalently, the very tiny effective capacitance of the dot). This switching off of the current is known as *Coulomb blockade*. A further increase in the gate voltage lowers the energy of the electron on the dot sufficiently that a second electron may enter the dot. This occurs when $E_F = E_0 + U$, where E_F is the Fermi energy in the lead, E_0 is the lowest energy in the well and U is the Coulomb repulsion energy between the two electrons on the dot. Since empty states are also available at energy E_F in the drain lead, an electron may leave the dot again, giving rise once more to a finite current. In this way we get a sequence of sharp spikes in the current vs gate voltage curve as shown in Fig. 4. We also point out that the Coulomb blockade is

still effective when there is a current flowing. The number of electrons on the quantum dot can be either N or $N + 1$ but other values are suppressed. An electron hopping onto the dot must leave it before another electron may enter. In this way the current is due to single electrons with mean spacing determined by the tunnelling time through the strongest barrier.

The quantum dots described above have some similarity with atoms in the sense that they usually have an integral number of electrons (Coulomb blockade mode) and there is an energy cost to either remove an electron (ionisation) or add an electron (affinity), as with atoms. Furthermore, the number of electrons on the dot may be changed by changing the Fermi energy. This is analogous to a change of valence of real atoms which may be effected by changing the local chemical potential. The analogy with atoms is somewhat closer for semiconductor dots than for metallic grains since the latter will typically contain many millions of conduction electrons whilst the former will usually have a small number, with $N = 0, 1, 2, \ldots$ corresponding to artificial $H^+, H, He, \ldots$ [8]. However, despite these similarities, there are important differences between real atoms and artificial atoms as we shall see in section IV.

III. CHARGING MODEL

There is a simple semi-classical model which explains with reasonable accuracy the behaviour of artificial atoms as described in the previous section [4]. Consider a metallic particle on an insulating surface to which we attach source leads via thin insulating (tunnel) barriers, as shown in Fig. 6. We introduce a positively charged 'gate' electrode close to the metal particle but sufficiently insulated from it that charge may may not tunnel. By applying a small bias between the leads we observe that the current shows oscillations with gate potential, similar to those of Fig. 4. A semi-quantitative explanation is as follows. Let the capacitance of the metal particle be C and the excess charge on it be Q. If the potential on the metal particle is V then the electrostatic energy is

$$E_Q = QV + \frac{Q^2}{2C} \tag{1}$$

where $Q = -Ne$ for an excess N of electrons. As V is increased, electrons will flow from the leads onto the dot, where the potential is lower (first term in Eq. (1)). However, opposing this is the large Coulomb repulsion between charges on the dot, represented by the small capacitance C (second term). At absolute zero, the total energy will be a minimum which, for this parabolic equation, gives $Q = -CV$. However, this is not quite correct since Q is not a continuous variable: the quantum dot must contain an integral number of electrons. N is thus the integer which makes E_{-Ne} closest to E_{-CV}. This is shown in Fig. 7a, where we also show the total energy with one extra electron and one fewer electron, corresponding to electron affinity and ionisation respectively. Denoting these energies by E_A and E_I, it follows directly from Eqn. (1) that

$$E_A + E_I = \frac{e^2}{C}$$

Furthermore, at $T = 0$ the current will be blocked for a very small potential difference between the leads due to the electron affinity and ionisation barriers. This is the Coulomb blockade which can, of course, be overcome at finite temperatures. Its effect is maximal when $E_A = E_I = \frac{e^2}{2C}$, as shown in Fig.7b, and minimal when there are two dot occupation numbers with exactly the same energy, as shown in Fig. 7c. For this latter case, there will be a "single-electron current" even at absolute zero. Hence, this simple model predicts current or conductance oscillations with equidistant peaks separated by $\Delta V = e/C$, which agrees approximately (though not precisely) with experiment. The model also explains the "Coulomb gap" shown in Fig. 1, which occurs when the gate voltage is held constant

3

but the voltage between the leads increased. Consider the arbitrary case shown in Fig. 7a. At absolute zero there will be no current for a potential difference less than E_A/e. If the potential on the left lead (say) is increased (i.e. the potential energy of electrons is lowered), then an electron in the dot will eventually have the same energy as the Fermi energy in the left lead and a one-electron current will flow from right to left. This will occur when the potential in the left lead has been raised by E_I/e. On the other hand, starting again with zero potential difference between the leads, if the potential on the right lead is decreased, an electron at the Fermi energy will be able to transfer to the dot with no energy penalty when the potential is $-E_A/e$ and a current will flow from right to left. Hence the potential difference between the onsets of left and right currents is

$$\Delta V = \frac{E_I + E_A}{e} = \frac{e}{C}$$

This relation can, of course, be used to estimate the effective capacitance in a two-terminal experiment. For observation at $4.2K$ or higher temperatures, this effective capacitance has to be very small, $\lesssim 10^{-17}F$.

IV. ENERGY SPECTRUM OF THE ARTIFICIAL ATOM - CORRELATIONS

The semiclassical charging model seems to provide a simple explanation of the main features of quantum dots and their similarity with atoms so do we only need to refine this theory to improve quantitatively the agreement with experiment? How far can we push the analogy of quantum dots as artificial atoms? Do they share other features of real atoms, such as a discrete energy spectrum, shell structure, Hund's rules etc.? There is now significant evidence, both theoretical and experimental, to support the view that there are some fundamental differences between real and artificial atoms. A simple analysis of the length and energy scales involved indicate that this might be the case. Within the parabolic-band effective-mass approximation, the natural units of energy and length are the scaled Rydberg and Bohr radius:

$$R_y^* = \frac{m^*}{m_0 \varepsilon^2} R_y, \ a^* = \frac{\varepsilon m_0}{m^*} a$$

These would be, for example, the ground-state binding energy and corresponding Bohr radius of a conduction electron bound to a shallow donor ion in a semiconductor. We show below, a table of these quantities for the semiconductors Si, GaAs and InSb, together with H for comparison.

	H	Si	GaAs	InSb
R_y^*(meV)	13,600	18	8	0.85
a^*(A)	0.529	33.4	82.4	567

We see that the energies are typically ~ 1000 times less than H with Bohr radii ~ 100 times greater! Furthermore, both with real atoms and shallow impurities in semiconductors, the length scale is dictated by the Coulomb attraction of the nucleus and the orbiting electrons. For atoms with more than one electron, this ensures that the kinetic energy remains greater than Coulomb repulsion energy between electrons. For example, in He the mean kinetic energy is almost three times the mean Coulomb repulsion energy between the two $1s$ electrons. For this reason, the independent electron approximation works very well for atoms. Hartree-Fock gives qualitatively the correct picture and even quantitatively errors are only about 5% for light atoms. For quantum dots, however, the situation can be quite different. Firstly the positive potential which confines electrons is usually much more gradual than the Coulomb potential of the atomic nucleus on the scale of the electron wavelength. For large dots, such as those produced by 'soft' confinement as

in systems fabricated on the basis of semiconductor heterojunctions, this will generally be parabolic. For 'hard' confinement, such as is produced by a heterojunction between two dissimilar semiconductors, the potential can be approximately constant inside the dot. Let us for simplicity consider two electrons in a quantum box with sides of length L and infinite barriers. The one-electron level spacing at low-energies due to kinetic energy is,

$$\Delta E_K \sim \frac{\hbar^2}{m^* L^2}$$

independent of dimensionality. On the other hand, the Coulomb repulsion energy between the two electrons is

$$E_C \sim \frac{e^2}{\varepsilon \varepsilon_0 L}$$

Hence

$$\frac{\Delta E_K}{E_C} \sim \frac{a^*}{L}$$

where we have used $a^* = \frac{\varepsilon \varepsilon_0 \hbar^2}{m^* e^2}$. This shows that for sufficiently large dots and given electron number, the Coulomb repulsion energy between electrons will dominate. For example, in a GaAs quantum dot, Coulomb effects are expected to dominate for $L > 0.15$ microns whereas in Si this would be about 500A. [1]. We will show in the next section how the relatively large Coulomb energy is expected to give rise to qualitatively different physics. This yields an energy spectrum for the artificial atom which is quite different from that given by the independent electron approximation, due to the correlations between electrons. However, in the very first experiments on small dots, where the excitation energies are expected to be sufficiently large to be observable, no deviation from the independent-electron picture was detected by means of (artificial) atomic (far infrared) spectroscopy [9]. The resolution of this paradox lies in a theorem due to Kohn [10], which states that the optical spectrum of an interacting electron system which is confined by a parabolic potential is independent of the interactions between electrons for dipole transitions. This is because the radiation field couples only to the centre-of-mass co-ordinate of all the electrons, the motion of which does not depend on electron-electron interactions. Although, strictly speaking, the confining potentials in quantum dots will not be perfectly parabolic, it turns out in practise that deviations from parabolicity are on the borderline of being observable which makes simple dipole excitations less favourite for probing correlation effects.

The other class of experiments are transport measurements of, for example, electrons tunnelling through a quantum dot in a single-electron transistor [7,11,12]. However, for the experiments described in Section II, which show oscillations in current vs gate voltage for very small source-drain voltage, we do not expect to see a dramatic effect of electron correlations either. This is because such experiments probe only the interacting ground-states of the quantum dot. The difference in ground-state energy when the number of electrons on the dot is changed by one in not very small quantum dots is accounted for with reasonable accuracy by the Coulomb charging model, which predicts a constant separation between peaks in the conductance oscillations. Nevertheless, in very recent experiments, where it has become possible to fabricate quantum dots containing down to $N = 1, 2, \ldots$ electrons and to contact them for transport experiments, significant deviations from the predictions of the simple model have been found, particularly for the first few peaks [13–16]. These deviations can be attributed to correlations. An even more significant probe

---

[1]This argument is a little too simplistic. For high confinement non-parabolicity effects in k-space and the finite height of the confining barriers can have a significant effect. Nevertheless these estimates are expected to be reasonable lower limits for the critical length scales beyond which Coulomb interactions dominate the physics.

would be to look at excited states. This can be done by simply increasing the source-drain voltage. In fact, by doing so we may regard the single-electron transistor as an *energy spectrometer* for quantum dots/artificial atoms! That such an experiment can probe the excited states of the quantum dot can be understood from the following argument, which closely follows that given at the end of Section III to explain the Coulomb gap. Suppose that at low temperature we adjust the gate voltage of the single-electron transistor just between two conductance oscillation peaks. Let there be N electrons on the dot. Suppose that the Fermi energy of the drain contact is now lowered by changing its voltage. Eventually the ground-state energy of the N electrons will be the same as the ground state energy of $N-1$ electrons on the dot plus an electron at the Fermi energy in the drain lead. This will cause a current to flow as an electron may leave the dot allowing another electron to enter it from the source lead. However, the *magnitude* of this current will depend strongly on the position of the Fermi energy in the source contact. If this is such that $E_F^{\text{source}} + E_{N-1}^0 < E_N^1$, where E_{N-1}^0 is the ground-state energy of the $N-1$ electrons on the dot and E_N^1 is the first excited state of N electrons on the dot, then the current will be due (only) to electrons in the source at energy $E_N^0 - E_{N-1}^0$ tunnelling into the dot. However, when $E_F^{\text{source}} + E_{N-1}^0 = E_N^1$ there are now two channels for tunnelling into the dot, *i.e.* electrons at the Fermi energy and electrons at energy $E_N^0 - E_{N-1}^0$. Hence, at this point there will be a sudden rise in current. These steps of increasing current occur whenever $E_F^{\text{source}} + E_{N-1}^0 = E_N^n$, where E_N^n is an excited state with N electrons. Hence there will be a fine structure at either side of the Coulomb gap reflecting the energy level structure of the dot [17,18]. This has indeed been observed in experiments that show a rich structure of resonance steps corresponding to excited states [19]. They also show some unusual features which cannot be explained by an independent-electron picture, such *negative differential resistance*. As we shall see in the next section, this kind of unusual behaviour is indeed expected for strongly correlated electrons on the quantum dot.

V. THEORY

It is well known that electrons interacting via Coulomb repulsion in a uniform background of positive charge behave quite differently in the high and low density limits. At relatively high densities comparable with that in real metals, the kinetic energy dominates and, despite the still large Coulomb repulsion, the system at low-energies may be mapped onto an independent-electron model of weakly interacting quasiparticles. [20] At low-densities this picture is not even qualitatively correct. The potential energy (Coulomb repulsion) dominates over kinetic energy and the electrons eventually form a lattice [21], with low-lying excitations that are lattice vibrations [22–24] (see also the article by Ando, Fowler and Stern [25]). This occurs for a mean separation between neighbouring electrons $\gtrsim 100 a_{\text{B}}$, where a_{B} is the effective Bohr radius (denoted by a^* in the previous section). For intermediate densities, this is an extremely difficult problem due to competing interactions from the quasi-classical 'lattice' vibrations and quantum mechanical exchange. Physical realisation of the Wigner lattice is an extremely challenging experimental problem due to the difficulty in obtaining a low-defect region with sufficiently low electron density. Nevertheless evidence of Wigner crystallisation has been reported in heterostructures [26,27].

With large quantum dots, we have the interesting possibility of the analogue of Wigner crystallisation for finite systems with just a few electrons [28]. In contrast to the infinite system, not only might the density–density correlation function crystallize but also the charge density distribution itself, with the electrons occupying energetically favourable positions within the dot. This can indeed be the case as we shall see, with the geometry of the confining region being crucial to the nature of the few-electron states in two and three dimensions. By analogy with the Wigner lattice, these quantum dot systems with large mean separation between electrons have been called Wigner molecules [29,30].

One theoretical advantage of studying few-electron systems is that they have the prospect of essentially being solved exactly by direct numerical diagonalisation of the Hamiltonian matrix [31]. It turns out that they are also amenable to approximations which are not valid for large systems (see below). Such approximations are still necessary, for although we are interested in a few-electron problem (with $N \lesssim 20$), it is prohibitively expensive on computer time to solve for more than a very few electrons by direct diagonalisation. For sufficient accuracy, the practical limit is $N = 5$ in one dimension and $N = 3$ in two dimensions. For high density systems we can, of course, get reasonable results with the independent-electron model using the Hartree-Fock approximation, for which solutions with tens of electrons are easily obtained [32]. However, this is a poor approximation when the mean electron separation is large and gives qualitatively incorrect results.

This may be seen from exact diagonalisations for a one-dimensional quantum dot with a simple rectangular well confining potential [33,30]. We summarise the main results of these computations in Figs. 8 and 9. Figure 8 shows the energy spectrum for $N = 1$ to 4 for a well width $L = 9.45a_{\mathrm{B}}$. This is seen to consist of a series of multiplets for which the energy separation between multiplets is much greater than the energy splitting within a multiplet. Furthermore we can easily see that this spectrum is qualitatively different from that which would be given by an independent-electron picture by examining the lowest multiplet with $N = 3$ electrons. In the independent-electron picture, we expect a doublet lowest followed further doublets at energies $\varepsilon_1 - \varepsilon_0$ and $\varepsilon_2 - \varepsilon_1$ (relative to the ground-state) and an octet at energy $\varepsilon_2 - \varepsilon_0$ etc., where ε_n are the one-electron levels. Instead we see a low-lying multiplet consisting of doublet, doublet, quartet with very small splitting between them ($\ll \varepsilon_1 - \varepsilon_0$), followed by a (relatively) very large gap to another multiplet of closely spaced levels. A clue as to what is causing this level structure is found in Fig. 9 where the charge density due to all three electrons in the ground-state of the interacting system is plotted for various L. These curves are qualitatively different for large and small L. For $L = 0.1a_{\mathrm{B}}$, we get a charge density characteristic of the independent-electron picture, since this would place two electrons in the nodeless ground-state and the third electron in the first excited state with a node at $L/2$, giving a shallow minimum in the total electron density. At the other extreme, with $L = 945a_B$, we see three distinct peaks. This is close to what we would expect in the 'Wigner limit', where the electrons arrange themselves with equal separation in order to minimise the electrostatic energy. This quasi-classical configuration is essentially spin-independent, as can be seen from the corresponding ground-state multiplet which is almost (but not quite) degenerate. These results are not unexpected. What is less obvious is the behaviour at smaller L, where we see a persistence of the Wigner picture down to rather small L, the three peaks being discernable even when $L = 1.9a_{\mathrm{B}}$ (*i.e.* mean electron separation of order a_{B})! Furthermore, an examination of the energy spectrum shows that the ground-manifold spin-multiplet, with $2^3 = 8$ states, remains well separated from higher-lying multiplets as L is reduced. The main effect is to increase rapidly the magnitude of the splitting within the ground-state multiplet as L is decreased whilst (approximately) preserving their ratio of order $2 : 1$. We see a similar behaviour for $N = 4$ with a ground-manifold spin-multiplet of dimension $2^4 = 16$, which splits into two singlets, three triplets and a quintet.

In the infinite system the low-lying excitations are sound waves in the Wigner limit when the spin can be ignored, since the electrons become distinguishable through their respective lattice sites. Indeed, this is what makes the problem prohibitively difficult at higher densities where the Fermi statistics of the electrons can no longer be ignored. The major simplification of the few-electron system is that these sound-wave-like excitations are high in energy compared to low-energy spin-splittings and can therefore be safely ignored [34], thus permitting the effect of the Fermi statistics to be examined in isolation as L decreases. This is similar to the situation in real molecules, where the separation between vibrational levels is greater than the fine-structure due to electron interactions. (Whereas in crystalline solids

7

both lattice vibrations and electronic excitations are present in the low-energy spectrum.)

In the remainder of this section we will concentrate mainly on the low-energy manifold of states for quantum dots in both one and two dimensions. Consider again the simplest non-trivial case of two electrons in a one-dimensional rectangular well, interacting via a potential of the form

$$V(|x_1 - x_2|) = \frac{e^2}{\varepsilon \varepsilon_0 \sqrt{(x_1 - x_2)^2 + \lambda^2}} \tag{2}$$

This has the usual Coulomb form for large separations between the electrons and passes through a maximum when the x–coordinates coincide. It models a quasi-1D quantum dot, the parameter λ representing the confinement in the other two dimensions, with λ decreasing as the confinement increases. We may regard this two-electron problem in 1D as a single-particle problem in 2D with momentum $\mathbf{p}=(p_1, p_2)$ and position $\mathbf{r}=(x_1, x_2)$. The potential landscape for this fictitious particle, $V(r)$, is shown in Fig. 10 where we see potential minima at $\mathbf{r} = (L, 0)$ and $(0, L)$, corresponding to the two positions where the 'real' particles (electrons) are maximally separated. When viewed in this way, the problem is reminiscent of a tunnelling problem in which the particle may start in one well, or 'pocket' and will subsequently tunnel to the other. To describe this situation quantitatively we may choose basis states for the particle in each well. These may be constructed, for example, by replacing the potential energy in region 2 of Fig. 10 by the maximum value $V_0 \equiv V(0) = \frac{e^2}{\varepsilon \varepsilon_0 \lambda}$ and solving for the eigenstates in region 1, $\psi_1^{(n)}$ say. Similarly for the well states in region 2, $\psi_2^{(n)}$. Now, if the barrier of the true potential (Fig. 10) is sufficiently strong then, to a good approximation, there will be two low-lying states

$$\psi_{\pm} = \frac{(\psi_1^{(0)} \pm \psi_2^{(0)})}{\sqrt{2(1 \pm s)}}$$

with corresponding energies

$$E_{\pm} = \frac{E_0 \pm t}{1 \pm s}$$

where $E_0 = \langle \psi_1^{(0)} | H | \psi_1^{(0)} \rangle = \langle \psi_2^{(0)} | H | \psi_2^{(0)} \rangle$, $t = \langle \psi_1^{(0)} | H | \psi_2^{(0)} \rangle$ and $s = \langle \psi_1^{(0)} | \psi_2^{(0)} \rangle$. Furthermore, these eigenstates will be well separated from higher-lying states. To complete the picture, we must impose the indistinguishability of the underlying electrons on these solutions. This is straightforward since we know that the symmetric solution, ψ_+, corresponds to a spin singlet and the antisymmetric solution, ψ_-, to a spin triplet.

The important point about the above analysis is that we may deduce the nature of the low-lying states without explicitly solving the problem, provided we can justify the neglect higher lying states in each well. This is indeed the case for the potential given in Eqn.2. It is emphasised that the base states themselves are highly correlated and cannot in general be approximated by a simple product of one-electron wavefunctions.

We may extend this 'pocket state' analysis to cases with more electrons and higher dimensions. Thus N electrons in D dimensions is equivalent to a single particle in a $N \times D$ dimensional space. This fictitious particle will move in a potential landscape with at least $N!$ minima corresponding to the classical minimum electrostatic energy of the N electrons regarded as distinguishable (though equivalent). In two and three dimensions there may be more minima for certain geometries. For example, consider 3 electrons in a square dot. The electrons will be repelled to the corners of the square and there will be four different configurations corresponding to one corner unoccupied and the remaining 3 occupied. Hence there will be $4 \times 3! = 24$ classical minima. In the general case there will be $\nu N!$ equivalent global minima. Provided these are well separated in energy from possible higher local minima then the structure of the low-lying eigenstates may again be deduced from the Hamiltonian matrix of the system within the basis of

the $\nu N!$ pocket states of lowest energy. For $N > 2$ the requirement that the true eigenstates be antisymmetric with respect to interchange of both position and spin is not trivial since, unlike the case of $N = 2$, the 'orbital' part of the wavefunction will be neither symmetric nor antisymmetric. However, the problem may be solved using the theory of permutation groups and the corresponding low-lying spectrum deduced [35,34].

The pocket state analysis suggests an alternative approach to the few-electron quantum dot problem which is similar to that used for strongly correlated lattice systems. The generic theoretical model for such lattice problems is the Hubbard model. This has been successful in modelling Mott insulators, the metal-insulator transition and, more recently, doped Mott insulators, which are believed to be relevant to the copper-oxide planes of high-temperature superconductors in which the physics is believed to be dominated by electron-electron correlations. [36] We can indeed show that this model is relevant to interacting electrons in a quantum dot but let us first review the main properties of the Hubbard model.

The Hubbard model is essentially a tight-binding model in which only the largest Coulomb matrix elements are retained. Consider, for example, a collection of one-electron atoms which are essentially in fixed positions but otherwise quite general (molecule, crystalline solid or disordered solid). Following Hubbard [37] we approximate this system by confining the Hilbert space to just one orbital per atom and drop all Coulomb matrix elements except the largest, which corresponds to two electrons of opposite spin on the same site (atom). The resulting Hamiltonian is

$$H = \sum_i \left(\varepsilon_i n_i + U_i n_{i\uparrow} n_{i\downarrow} \right) + \sum_{\langle ij \rangle \sigma} \left(t_{ij} c_{i\sigma}^\dagger c_{j\sigma} + \mathrm{H.c.} \right) \tag{3}$$

where $n_i = n_{i\uparrow} + n_{i\downarrow}$, $n_{i\sigma} = c_{i\sigma}^\dagger c_{i\sigma}$, ε_i is a one-electron energy for atom i, t_{ij} is a hopping matrix element from atom i to atom j and U_i is a Coulomb matrix element for two electrons on atom i. In this equation, the angular brackets in the summation over i and j denotes pairs of atomic sites in which each pair is counted only once. The one-electron wavefunction on atom i is $\psi_i(\mathbf{r}) \chi_\sigma \equiv \langle \mathbf{r} | c_{i\sigma}^\dagger | \mathrm{vac} \rangle$ and

$$\varepsilon_i = \langle \psi_i | \left[\frac{\mathbf{p}^2}{2m} + v(\mathbf{r}) \right] | \psi_i \rangle,$$

$$t_{ij} = \langle \psi_i | \left[\frac{\mathbf{p}^2}{2m} + v(\mathbf{r}) \right] | \psi_j \rangle,$$

$$U_i = \int |\psi_i(\mathbf{r})|^2 |\psi_i(\mathbf{r}')|^2 \frac{e^2}{|\mathbf{r} - \mathbf{r}'|} \mathrm{d}^3 r \mathrm{d}^3 r'$$

where $v(\mathbf{r})$ is some (optimal) one-electron pseudopotential. In some situations (for example when there is significant charge transfer from one atom to another) the Coulomb interaction between electrons on different atoms can be important and we have to add the term

$$\sum_{\langle ij \rangle} V_{ij} n_i n_j \tag{4}$$

to Eq. (3), where

$$V_{ij} = \int |\psi_i(\mathbf{r})|^2 |\psi_j(\mathbf{r}')|^2 \frac{e^2}{|\mathbf{r} - \mathbf{r}'|} \mathrm{d}^3 r \mathrm{d}^3 r'$$

The resulting Hamiltonian is sometimes referred to as the extended Hubbard model. When the separation between the atoms is sufficiently large, which is the regime of interest to us here, it follows that the $t \ll U$, for all t and U.

This is known as the strongly correlated regime since the motion of the electrons are strongly dependent on each other and is truly a many-body problem. (The amplitude for an electron to hop from one atom to another is strongly dependent on whether the recipient atom is occupied or not because of the large U.) Despite this being a difficult problem, a certain simplification arises in this strong correlation regime as many of the states in the many-electron Hilbert space may be eliminated by perturbation theory in t/U or, equivalently, a canonical transformation. [38–41]

For the important case in which the number of electrons equals the number of atoms, it may be shown that the low-energy states of H are given by an effective spin model in which each atom always has one electron but electrons (spins) on neighbouring sites interact via an antiferromagnetic Heisenberg exchange interaction, *i.e.* the effective Hamiltonian

$$H_{\text{eff}} = \sum_{\langle ij \rangle} J_{ij} \mathbf{s}_i \cdot \mathbf{s}_j \tag{5}$$

has, apart from an unimportant constant energy shift, the same low-energy spectrum (to second-order) as the original Hamiltonian, H. In this equation the positive exchange interactions J_{ij}, often referred to as superexchange, are given by

$$J_{ij} = 2|t_{ij}|^2 \left[\frac{1}{U_i} + \frac{1}{U_j} \right]$$

(This gives a total exchange for a pair of atoms of $J\mathbf{s}_i \cdot \mathbf{s}_j$ where $J = 4|t|^2/U$ for a homogenous system.) This reduction to a Heisenberg spin model simplifies the Hubbard models in two ways. Firstly, it drastically reduces the size of the Hilbert space since each site can be in one of only two states compared with four for the Hubbard model. Secondly, it gives a new language and insight to describe the low-energy spectrum.

When the number of electrons does not equal the number of atoms this means some sites must be unoccupied ($N_e < N_s$) or doubly occupied ($N_e > N_s$), even in the low-energy manifold. In fact, these two regimes are related to each other by electron-hole symmetry so we need only consider one, $N_e < N_s$ say. For this regime states involving double occupations are high in energy and, as with the case $N_e = N_s$ above, may be eliminated by perturbation theory leading to an effective Hamiltonian for the low-energy manifold:

$$H_{\text{eff}}^{tJV} = P \sum_{\langle ij \rangle} \left[\sum_{\sigma} (t_{ij} c_{i\sigma}^\dagger c_{j\sigma} + \text{H.c.}) + J_{ij}(\mathbf{s}_i \cdot \mathbf{s}_j - 1/4) n_i n_j + V_{ij} n_i n_j \right] P \tag{6}$$

In this effective Hamiltonian the operator P is a projection operator which precludes all many-electron states in which sites are doubly occupied. In the strong correlation regime, $t \gg J$, since $J \backsim t^2/U$ and $U \gg t$, and hence we may drop the J-term in (6) if we neglect energy separations on the scale of J. The resulting t−model would be a simple one-electron tight-binding model were it not for the P-operators. These make the model much more difficult to solve and can give rise to unusual effects related to correlation implicit in P. For example, a homogeneous system (lattice) with one 'hole' (*i.e.* $N_s - 1$ electrons) has a ground state of maximum spin. [42]

To relate the low-density interacting-electron problem in a quantum dot to the Hubbard model we start by approximating the pocket states by products of one-electron states, $\psi_i(\mathbf{r})$, centred about 'sites' i that define the electrostatic ground-state energy. This is not an unreasonable approximation provided that the one-electron states are chosen optimally, which requires them to be non-orthogonal. With such a choice we could form a set of antisymmetrized basis functions (Slater determinants) for the N electrons by forming spin-orbitals, $\psi_i(\mathbf{r})\chi_{i\sigma}$, and antisymmetrizing products of N such spin-orbitals, with the constraint that no more than one electron shall occupy one 'site'. It may

be shown that there is precisely a one-to-one mapping between these base states and corresponding permutation-symmetry adapted pocket states, the total number being 2^N for the (usual) case when the number of electrons equals the number of 'sites'. [34] (An exception to this is considered below.) However, such a procedure is complicated by the non-orthogonality of the one-electron states. We can circumvent this problem and actually improve on the approximation by orthogonalising the one-electron orbitals and expanding the Hilbert space to allow any site to be occupied by either zero, one or two electrons (subject, of course, to the constraint that the total number of electrons be N). If we now express the Hamiltonian of the quantum dot (*cf* Eqn. (2))

$$H_{\mathrm{dot}} = \sum_{i=1}^{N} \left[\frac{\mathbf{p}_i^2}{2m^*} + v(\mathbf{x}_i) \right] + \sum_{\langle i,j \rangle} \frac{e^2}{\varepsilon \varepsilon_0 \sqrt{(\mathbf{x}_i - \mathbf{x}_j)^2 + \lambda^2}}$$

in this expanded basis set of Slater determinants we get, in second quantized form, the Hubbard model Eq. (3), including the intersite interaction Eq. (4). [43]

Having established this equivalence of the quantum dot problem to a Hubbard model we may deduce properties of the low-energy spectrum for various cases. In one-dimension we can transform the Hubbard model into a Heisenberg model for the quantum dot. This is because the electrons will always arrange themselves to form a 'lattice' (chain) in which the number of lattice sites equals the number of electrons. The lattice sites will, of course, be determined by the electrons themselves. For example, in a rectangular well of width L the lattice will be uniform with spacings $L/(N-1)$ in the Wigner limit. This should be contrasted with a chain of atoms for which the number of lattice sites and their spacings are independent of electron number. We have calculated the low-energy spectrum of one-dimensional quantum dots with up to six electrons using the Heisenberg model and confirmed that the results agree precisely with the pocket state method and, where applicable, exact results. This also explains the nature of the lowest spin-multiplets obtained by direct diagonalisation and described earlier in this section. In all cases in one dimension, the ground-state is always low-spin in accordance with the Lieb-Mattis theorem. [44]

The equivalence between interacting electrons in a quantum dot and a Hubbard model has important and interesting consequences in higher dimensions. These arise for two reasons: (i) the number of 'sites' may exceed the number of electrons and (ii) the ground state need not necessarily be low-spin. We will now consider these in more detail.

Case (i) is the analogue of the doped Mott insulator for lattice models and is described by the tJV-model, Eq. (6). For the quantum dot, the exchange parameters J_{ij} are relatively very small and on the scale of t and V they may be dropped. In some cases the V may also be dropped since it merely gives rise to an overall energy shift. For example, three electrons in a two dimensional quantum dot of square symmetry. There are four positions for the 'hole' in this system, as shown in Fig. 11, and all have the same contribution from the V-term. Dropping these and the J-term in Eq. (6) we are left only with the t-term, like a simple tight-binding model. However, as stated earlier the presence of the projection operators, P, have an important effect and the analytic solution of the problem shows that the ground state is one of high-spin, *i.e.* a spin polarised state (see Fig.12a). This is purely an interference effect in that the hole may gain maximum kinetic energy when all spins are aligned and is the analogue of the spin-polarised state for a single hole in a lattice system. [42].

A situation where the V-term *is* important is that of two electrons in a square well in two dimensions, as shown in Fig. 13. The first two states are lower in energy by an amount $V = V_{12} - V_{13}$ and the two electrons are repelled to opposite corners along the diagonals. Although it is straightforward to diagonalise the Hamiltonian matrix with all 6 base states (24 including spin), we may obtain the lowest states by perturbation theory and the system will resonate between the two low-energy base states with amplitude $\Delta = 2t^2/V$. This is described by the effective Hamiltonian (given by degenerate perturbation theory)

$$H_{\text{eff}} = \Delta(n_1 n_3 - n_2 n_4)(R_{\pi/2} - R_{-\pi/2}) + J\left[(\mathbf{s}_1 \cdot \mathbf{s}_3 - 1/4)n_1 n_3 + (\mathbf{s}_2 \cdot \mathbf{s}_4 - 1/4)n_2 n_4\right] \tag{7}$$

where R_θ is a rotation operator, *i.e.*

$$R_{\pi/2}|\sigma, *, \sigma', *\rangle = |*, \sigma, *, \sigma'\rangle \quad ,$$

etc. Note that the prefactor $(n_1 n_3 - n_2 n_4)$ takes the value ± 1 depending on whether either 'sites' 1 and 3, or 2 and 4 are occupied. This effective Hamiltonian is easily diagonalised. The spectrum consists of two singlets and two triplets. We see immediately that (7) gives zero when operating on a spin-polarised state and hence the triplets are at zero energy with the singlets at energies $-J \pm 2\Delta$, in agreement with what is obtained from the pocket state approximation for this problem when the exchange of the two electrons is included there [35]. There are thus two contributions to the 'binding energy' of the singlet ground state, a resonance energy (-2Δ) and a superexchange energy $(-J)$. It is easy to see that the former will be dominant since it occurs in second-order and does not involve double-occupation of a 'site'. On the other hand, there are two contributions to J, the second-order term $\sim 4t_{13}^2/U$ and fourth-order terms $\sim t_{12}^4/V^2 U$.

The cases of four and five electrons on a square reduce directly to an effective Heisenberg model and the corresponding spectra are shown in Fig. 12b and 12c. We note that the ground-state of $N = 4$ has $S = 0$ whereas for $N = 5$ the ground has $S = 3/2$, *i.e.* not the low-spin ground state. This is easily understood from the Heisenberg model which, due to the antiferromagnetic exchange interaction, will tend to align adjacent spins antiparallel. With 4 electrons this gives $S = 0$ but with 5 electrons the spin on the electron in the centre of the square will tend to align antiparallel with those in the four corners, giving $S = 3/2$. (Note that the exchange interaction between electrons on neighbouring corners will oppose this tendency to parallel alignment but, since the distance is a factor $\sqrt{2}$ greater than to the centre, this 'frustration' is insufficient to enforce low-spin.)

This difference in the nature of the ground states for 4 and 5 electrons in a square dot has important consequences for single-electron transport. This is shown in Fig. 14 where we consider a situation where the ground state energy of the dot with 5 electrons is exactly degenerate with that of 4 electrons in their ground state and one electron at the Fermi energy in a lead. (We assume that the source-drain voltage is vanishingly small.) Strictly speaking, these states cannot be connected by a tunnelling interaction at $T = 0$ since this is forbidden by conservation of spin, *i.e.* to be allowed the total spin S on the dot may only differ by $\pm 1/2$ when the electron number fluctuates by one. This phenomena is known as *spin blockade* [45] since, if we imagine starting in the Coulomb blockade regime with 4 electrons on the dot in their ground-state with energy $E_4 < E_5 - E_F$ (where E_5 is the ground-state energy with 5 electrons), and raise the energy of E_4 (via the gate voltage), then the current through the dot will be spin-blocked even when $E_4 + E_F = E_5$. By further raising the energy of the electrons on the dot relative to the Fermi energy, the single-electron current will eventually be 'switched on' when the $S = 1/2$ states with 5 electrons become degenerate with $E_4 + E_F$. A finite conductance may also be recovered from the spin-blockade regime by either raising the temperature, when excited states with $S = 1/2$ again become involved, or by increasing the source-drain voltage, which has a similar effect. These effects are generic in the sense that they will apply to a variety of quantum-dot geometries (either contrived or accidental). In this way the 'recovery' of 'missing' conductance peaks when heating the sample up to 500 mK, as observed in [46], can be interpreted by such a spin blockade phenomenon [47].

Although the above equivalence of a few-electron quantum-dot system to Hubbard/charge-spin models is adequate for most situations, there is one further class of problem for which it breaks down. These are problems with very high symmetry in which processes involving the simultaneous movement of more than two electrons can be important or even dominant in comparison to processes where just two neighbouring electrons are exchanged. A simple example

would be an (almost) circular dot that contains a very small number ($N = 2 \ldots 6$) of electrons and is sufficiently large that the mean separation between electrons exceeds the Bohr radius. In the classical Wigner limit there are low-energy states in which all N electrons arrange themselves around the periphery of the dot and rotate whilst preserving their relative separations. This indicates that the corresponding elementary permutational process, a cyclic exchange of all electron places, is connected with a larger probability amplitude than the exchange of two nearest neighbours. This affects considerably the spin multiplets at low energies. For example, an odd electron number favours a high-spin ground-state while $S = 0$ for N even. Another example where 'higher order' permutations processes could be important is inside the bulk of an extended Wigner crystal (or, a large dot containing many electrons at low-density) where the electrons arrange themselves in the form of an (almost) hexagonal lattice. There, $2\pi/3$ rotations of any of the electron triangles composing the lattice could well be of similar importance to the pair exchange of adjacent electrons.

Can the Hubbard/charge-spin models be modified to accommodate these processes? The answer is yes and in fact similar processes can also be important for lattice systems, though this is not well-kown. An example of the latter is a contribution to the superexchange between two holes in the copper-oxide planes of the high temperature superconductors in which the holes never occupy the same sites simultaneously. [48] For the quantum dot, we may illustrate these processes by considering a triangular quantum dot. By introducing intermediate lattice points, we can rotate all 3 electron through $2\pi/3$ in a series of 6 steps as shown in Fig. 15. The intermediate steps are higher in energy than the initial and final states (the electrostatic Coulomb energy is higher) and may be eliminated by perturbation theory. The result is an effective interaction of the form $-K(R_{2\pi/3} + R_{-2\pi/3})$, where K is a constant energy and $R_{2\pi/3}$ ($R_{-2\pi/3}$) is an operator which performs a cyclic (anticyclic) rotation of all three electrons. We note that these rotation operators may be written as spin-operators using the identities,

$$R_{2\pi/3} \equiv P_{12}P_{23} \text{ and } R_{-2\pi/3} \equiv P_{23}P_{12}$$

where $P_{ij} \equiv 2\mathbf{s}_1 \cdot \mathbf{s}_2 + 1/2$ is the Dirac exchange operator. Hence, expressing the exchange term in Eq. (6) in terms of these permutation operators and dropping an overall constant energy, the effective spin-Hamiltonian for 3 electrons in an equilateral triangular potential well becomes,

$$H_{\text{eff}} = \frac{J}{2}\left[(P_{12} - 1) + (P_{23} - 1) + (P_{31} - 1)\right] - K(P_{12}P_{23} + P_{23}P_{12}) \quad .$$

We see immediately from this form that the spin polarised state has eigenenergy $-2K$. It is straightforward to complete the diagonalisation of H_{eff} which results in a further pair of degenerate doublets at energy $K - 3J/2$. We refer to the K-term as a 'ring' term and we see that it opposes the exchange (J) terms, with the former favouring a high–spin ground state and the latter a low–spin ground state. The crossover occurs at $J = 2K$, which is not quite reached for the equilateral triangle, as discussed above.

This will not always be so for other geometries as follows immediately from the fact that we can change the shape of the dot in such a way that the ring processes are increased in amplitude relative to the exchange processes, as shown, for example, in Fig. 16b. An 'extreme' example of this is the circular dot (Fig. 16c) which, as discussed earlier, has a spin polarised ground-state ($S = 3/2$). The transition from high-spin to low-spin ground states in rings with increasing impurity barrier has been discussed recently in the context of persistent currents. [49]

In summary, we have shown in this section how the low-density few-electron problem in a quantum dot may be mapped onto a Hubbard model and that this may be further reduced to a charge-spin model. In one dimension we always get an effective Heisenberg model with antiferromagnetic exchange and a low-spin ground state. In higher

dimensions there are other possibilities which depend upon dot geometry and the number of electrons. This can have a dramatic effect on the nature of the energy spectrum, both for the ordering of the states and the energy scale of the separations between levels. For geometries in which there is only one electrostatic configuration in the classical limit, the degeneracy due to the permutation of electrons on different 'lattice sites' is partly lifted by quantum mechanical exchange described by an antiferromagnetic Heisenberg model. In this cases there is just one energy scale for the splitting between multiplets, the exchange energy J. Note, however that in more than one dimension the ground state spin can be larger than minimum, an example being 5 electrons in a square. In other situations, where there is more than one classical electrostatic configuration of lowest energy, the energy separations of multiplets may be quite different. For example, for 3 electrons (1 hole) in a square there will be energy splittings on both the scale of t and of J, with $t \gg J$ and, furthermore, the ground-state will be high spin. The so-called 'ring' processes can also be important. These effectively represent the simultaneous cyclic permutation of more than two electrons and have a characteristic energy scale K. For the example of 3 electrons in a triangle, K approaches the rotational constant $h^2/6mL^2$ of a perfect circular dot of circumference L, as the triangle is distorted into a circle, when there will be energy spilittings on the scale of both K and J, with a crossover from low-spin to high-spin ground state. More complicated situations can be envisaged as the number of electrons is increased. Thus, for example, 7 electrons in a square dot will have a classical ground-state configuration with four electrons in the corners of the dot and the remaining three forming a triangle in the interior of the dot. Important quantum mechanical processes will include pair exchange and 'ring' processes in which the three interior electrons will perform 'rigid' rotations of $\pi/6$. Future work could investigate these processes in more detail and estimate their relative magnitudes using quasi-classical methods, in addition to investigating other geometries which show promise for device applications.

VI. FUTURE PROSPECTS

The science of quantum dots and artificial atoms is still very much in its infancy and we can expect many new developments in the forthcoming years as technological advances permit reliable and reproducible fabrication of device structures. From the present perspective, a number of areas with both fundamental and applications potential seem worthy of further investigation.

Single dots which are not too small offer the possibility of investigating in a controlled way both the Wigner 'lattice' and the transition from the Wigner regime to the independent electron (quasiparticle) regime as the electron number and mean electron density is increased. As disussed in the previous section, the fundamental difference between the Wigner regime in a 'few-electron' quantum dot and the infinte Wigner lattice is the major effect of the boundaries that can increase the ground state spin to values greater than $S = 0$ or $S = 1/2$, and provides a separation of the energy scales related to 'vibrational' and spin degrees of freedom, respectively. In principle, this opens two possible scenarios towards the Wigner transition. Firstly, we can increase the system size whilst maintaining a sufficiently low but constant density to bring the excited vibrational states closer to the ground manifold. They eventually will mix with the spin states which changes the low energy physics qualitatively. On the other hand, we can imagine to increasing the confinement with a constant number of electrons. This will suppress the (effective) spin dependence of the low energy states and leave the quantum dot with classical electrons, in analogy to the transition from the Heitler-London to the molecular orbital picture in molecules. This crossover is also related to the metal-insulator (Mott) transition which can take place in strongly correlated lattice systems.

Another area worthy of further investigation is the magnetic field dependence in the Wigner regime. Large magnetic

14

fields modify the low energy eigenstates considerably [50], as it is observed also experimentally in quantum dots [51–53,16]. However, as a pure quantum effect even a non-vanishing vector potential (which does not require a magnetic field at the location of the electrons at all) can have very interesting consequences. One famous example is that of finite currents circulating around a small ring due to the Aharonov–Bohm flux ϕ enclosed by the ring (which is an equilibrium effect, in contrast to superconducting currents !). It is known that electron–electron interactions are important, otherwise the experimentally observed magnitudes of the currents cannot be understood. Theoretically, this problem can be approached by considering a one-dimensional quantum dot, such as that described in Section V, deforming it to form a ring. The electron molecule can then rotate (almost) freely, maintaining the distances between the electrons. The ground state energy E_0 and, most importantly, the ground state spin S, can then be determined in a similar way to that described in Section V [49]. However, they depend now on ϕ. This determines the persistent current that is proportional to the derivative $\partial E_0(\phi)/\partial \phi$ (at zero temperature). Since even impurities along the ring do not cause level repulsion between energies belonging to different spin values S and S', the persistent current can exhibit discontinuous jumps near values for the flux where level crossings occur. In disordered rings this would not occur for spinless electrons. The magnitude of the persistent current indeed increases with increasing interaction strength. The main shortcoming of this model of a very thin, one-channel ring is that it cannot explain values of the current observed experimentally, which correspond to almost freely circulating electrons. [54]. However, it has became clear that maximum persistent currents in disordered rings require the investiation of wider, many channel rings. For any description within the picture of Wigner localized electrons this means that we need to increase the electron number in the ring considerably. This is only feasible using an approach that is highly selective in the Hilbert space describing the low-energy physics. The spin-charge representation described in Section V should provide a means of achieving this.

There are many new effects to be investigated in multiple quantum dots and quantum dots arrays, *i.e.* artificial molecules and solids. Unlike their 'real' counterparts, they have the prospect of being controlled in a well defined way as technology advances. Thus, for example, we have the prospect of studying the classic Mott transition [55] for an array of one-electron artificial atoms as the ratio of the tunnelling matrix element between dots to the Coulomb charging energy is varied. Another way of inducing a metal-insulator transition is to change the number of electrons on each artificial atom by simply varying the chemical potential through gate voltages. The insulator to metal transition occurs when the Fermi energy exceeds the minimum tunnelling barrier between dots and a dot array becomes an 'antidot' array. [56] The 'insulating' regime of such an array of one-electron artificial atoms would be interesting in its own right since, as with real atoms, we might expect an antiferromagnetic superexchange interaction between neighbouring dots. With more electrons/dot we could 'engineer' artificial atoms with high-spin ground states (by choice of dot geometry and electron number). These would give rise to magnetic correlations between dots and could, in principle introduce magnetic low energy modes and, eventually, magnetically ordered phases at sufficiently low temperatures. More generally, in the long-term we can invisage 'designer' molecules and solids with desired properties (energy structure, band structure, conductivity, susceptibility, anisotropy etc.)!

Finally, we may speculate on the feasibility of practical applications of quantum dots, single-electron transistors etc. The main obstacle to their widespread use for electronic applications is the need for low-temperatures. The temperature scale is ultimately set by the size of the quantum dot and, in principle, there is no fundamental reason why devices should not be made sufficiently small to operate at room temperature or higher. Indeed, there has been a great deal of progress over the past five years during which we have seen the temperature of operation of single-electron transistors increase from 4K to 77K, with evidence for oscillations in conductance due to single-electron

tunnelling being discernible even at room temperature. [57] Similar evidence for room-temperature, single-electron memory devices has also been reported recently. [58] There is little doubt that this progess will continue with the relentless drive towards smaller structures as nanoelectronics approaches the molecular level. With the need for ever increasing levels of integration and low-power consumption there is also little doubt as to the potential markets for single electronics, though the formidable technological problems associated with reproducibility and fabrication on the nanoscale should not be underestimated. Other promising areas for quantum dot arrays and quantum wires are optical applications, particularly low-threshold lasers. Here again the key issues at present are technological, with the need to reproduce devices with a small variance in size. Despite these difficulties, recent progress is encouraging and prospects are good for the use of quantum dots and artificial atoms to investigate fundamental physics and the development of new device concepts into the twenty-first century.

Acknowledgements

[1] R. P. Feynman, *Quantum Mechanical Computers,* Optics News **11**, Optical Soc. Am. 11-20 (1985).

[2] M. A. Kastner, Rev. Mod. Phys. **64**, 849 (1992), Physics Today **46**, 24 (1993).

[3] D. Pfannkuche, V. Gudmundsson, and P. A. Maksym, Phys. Rev. B **47**, 2244, (1993).

[4] D. V. Averin and K. K. Likharev, J. Low Temp. Phys. **62**, 345 (1986).

[5] M. H. Devoret, *et al.*, Phys. Rev. Lett. **64**, 1824 (1990);
For overviews cf. H. Grabert and M. Devoret, editors, *Single Charge Tunneling,* NATO ASI Series, Volume 294, Plenum Press (1992) and references therein;
and
G. Schön and A. D. Zaikin, Physics Reports **198**, 237 (1990).

[6] R. P. Andres *et.al.,* Science **272**, 1323 (1996).

[7] U. Meirav *et.al.,* Z. Phys. B **85**, 357 (1991).

[8] B. Meurer, D. Heitmann, and K. Ploog, K., Phys. Rev. Lett. **68**, 1371 (1992);
R. C. Ashoori, *et al.*, Phys. Rev. Lett. **68**, 3088 (1992);
Cf. also the overviews by D. Heitmann and J. P. Kotthaus, Physics Today **56** (June 1993); U. Merkt, Physica B **189**, 165 (1993).

[9] Ch. Sikorski and U. Merkt, Phys. Rev. Lett. **62**, 2164 (1989).

[10] W. Kohn, Phys. Rev. **123**, 1242 (1961); A. O. Govorov and A. V. Chaplik, JETP Lett. **52**, 31 (1990).

[11] L. P. Kouwenhoven *et al.*, **85**, 367 (1991).

[12] T. Heinzel *et al.*, Europhys. Lett. **26**, 689 (1994);
cf. also L. J. Geerligs, C. J. P. M. Harmans, and L. P. Kouwenhoven, editors, *The Physics of Few–Electron Nanostructures*,
North Holland, Physica B **189** (1993) for more details.

[13] S. Tarucha *et al.*, Phys. Rev. Lett. **77**, 3613 (1996).

[14] U. Sivan *et al.*, Phys. Rev. Lett. **77**, 1123 (1996).

[15] F. Simmel, T. Heinzel, and D. A. Wharam, preprint (1996).

[16] N. B. Zhitenenv *et al.*, preprint (1997).

[17] D. V. Averin, A. N. Korotkov, and K. K. Likharev, Phys. Rev. B **44**, 6199 (1991).

[18] C. W. J. Beenakker, Phys. Rev. B **44**, 1646 (1991).

[19] A. T. Johnson *et al.*, Phys. Rev. Lett. **69**, 1592 (1992);
E. B. Foxman, *et al.*, Phys. Rev. B **47**, 10020 (1993);
J. Weis *et al.*, Phys. Rev. Lett. **71**, 4019 (1993); Semicond. Sci. Technol. **9**, 1890 (1994).

[20] L. D. Landau, Soviet Physics JETP, **35**, 70 (1959).

[21] E. P. Wigner, Phys. Rev. **46**, 1002 (1934).

[22] A. V. Chaplik, Sov. Phys. JETP **35**, 395 (1972).

[23] G. Meissner, Z. Phys. B **23**, 173 (1976).

[24] I. M. Tsidil'kovskiĭ, Usp. Fiz. Nauk **152**, 583 (1987).

[25] T. Ando, A. B. Fowler, and F. Stern, Rev. Mod. Phys. **54**, 437 (1982).

[26] V.B. Timofeev, in *Optical Properties of Semiconductors*, ed. by G. Martinez, ASI, Kluwer Academic Publishers, 1993.

[27] R.G. Clark, Physica Scripta T **39**, 45 (1991).

[28] *Cf.* the study by V. M. Bedanov and F. M. Peeters, Phys. Rev. B **49**, 2667 (1994) for classical electrons.

[29] P. A. Maksym, Physica B **184**, 385 (1993).

[30] K. Jauregui, W. Häusler, and B. Kramer, Europhys. Lett. **24**, 581 (1993).

[31] G. W. Bryant, Phys. Rev. Lett. **59**, 1140 (1987);
U. Merkt, J. Huser, and M. Wagner, Phys. Rev. B **43**, 7320 (1991);
P. Hawrylak and D. Pfannkuche, Phys. Rev. Lett. **70**, 485 (1993).

[32] V. Gudmundsson and R. R. Gerhards, Phys. Rev. B **43**, 12098 (1991).

[33] W. Häusler and B. Kramer, Phys. Rev. B **47**, 16353, (1993).

[34] W. Häusler, Z. Phys. B **99**, 551 (1995).

[35] W. Häusler, in *Advances in Solid State Physics*, Vol 34, ed. by R. Helbig, Vieweg, Braunschweig (1994).

[36] E. Dagotto, Rev. Mod. Phys. **66**, 763 (1994) and references therein.

[37] J. Hubbard, Proc. Royal Soc. London **A 276**, 238 (1963).

[38] I. Lindgren, J. Phys. B: At. Mol. Phys. **7**, 2441 (1974).

[39] J. H. Jefferson, J. Phys. C **21**, l193 (1988).

[40] J. R. Schrieffer, P. A. Wolff, Phys. Rev. **149**, 491 (1966).

[41] K. A. Chao, J. Spalek, A. M. Oles, Phys. Rev. B **18**, 3453 (1978).

[42] Y. Nagaoka, Phys. Rev. **147**, 392 (1966).

[43] J. H. Jefferson and W. Häusler, Phys. Rev. B **54**, 4936 (1996).

[44] E. Lieb, D. Mattis, Physical Review **125**, 164 (1962).

[45] D. Weinmann, W. Häusler, W. Pfaff, B. Kramer, U. Weiss, Europhys. Lett. **26**, 467 (1994); Z. Phys. B **96**, 201 (1994);
D. Weinmann, W. Häusler, K. Jauregui, B. Kramer p. 297 in 'Quantum Dynamics of Submicron Structures, ed. by
H. A. Cerdeira, B. Kramer, G. Schön, NATO ASI Series E, Applied Sciences, Vol. 291, Kluwer, Dordrecht (1995);
D. Weinmann, W. Häusler, B. Kramer, Phys. Rev. Lett. **74**, 984 (1995).

[46] J. T. Nicholls *et al.*, Phys. Rev. B **48**, 8866 (1993);
A. M. Chang *et al.*, Phys. Rev. Lett. **76**, 1695 (1996).

[47] D. Weinmann, W. Häusler, B. Kramer, Annalen der Physik **5**, 652 (1996).

[48] H. Eskes and J. H. Jefferson, Phys. Rev. B **48**, 9788 (1993).

[49] W. Häusler, B. Kramer p. 169 in 'Quantum Dynamics of Submicron Structures, ed. by H. A. Cerdeira, B. Kramer, G. Schön,
NATO ASI Series E, Applied Sciences, Vol. 291, Kluwer, Dordrecht (1995);
W. Häusler, Physica B **222**, 43 (1996).

[50] V. Fock, Zeitschr. Phys. **47**, 446 (1928).

[51] P. L. McEuen *et al.*, Phys. Rev. Lett. **66**, 1926 (1991).

[52] R. C. Ashoori *et al.*, Phys. Rev. Lett. **71**, 613 (1993).

[53] J. Weis, R. J. Haug, K. v. Klitzing, and K. Ploog, Semicond. Sci. Technol. **9**, 1890 (1994).

[54] V. Chandrasekhar *et al.*, Phys. Rev. Lett. **67**, 3578 (1991);
D. Mailly, C. Chapelier, and A. Benoit, Phys. Rev. Lett. **70**, 2020 (1993).

[55] N. F. Mott, Proc. Phys. Soc. A **62**, 416 (1949); Can. J. Phys. **34**, 1356 (1956); Phil. Mag. **6**, 287 (1961).

[56] R. Fleischmann *et. al.*, Phys. Rev. Lett. **68**, 1367 (1992).

[57] Y. Takahashi *et. al.*, Elec. Lett. **31**, 136 (1995); K. Murase *et. al.*, Microelectronic Engineering 28, 399 (1995).

[58] A. Nakajima *et. al.*, IEDM 96, 952 (1996); L. Guo *et. al.*, IEDM 96, 955 (1996).

Figure Captions

FIG. 1. Current *vs* voltage for a small metal particle, showing the 'Coulomb gap'.

FIG. 2. Schematic diagram of a single-electron transistor.

FIG. 3. Electron potential-energy landscape in the plane of the two-dimensional electron sheet of the single-electron transistor of Fig. 2.

FIG. 4. Current *vs* gate voltage for a single-electron transistor with small souce-drain bias, showing single-electron Coulomb oscillations.

FIG. 5. Potential landscape for the single-electron transistor showing (a) empty quantum well with no current at $T = 0$ and (b) quantum well occupied with finite current at $T = 0$.

FIG. 6. Schematic diagram of small metal particle on an insulating substrate with source, drain and gate leads.

FIG. 7. Energy parabolas for the semi-classical charging model. The bullets indicate the possible values for the metallic island. (a) arbitrary gate voltage showing quasi-atomic ionisation energy (E_I) and electron affinity (E_A). (b) situation mid-way between two successive conductance peaks (c) situation right at a conductance peak.

FIG. 8. Typical spectra of square well model in 1D for $N = 1, \ldots, 4$ and $L = 9.45a_\mathrm{B}$. For $N \geq 2$ the low-lying eigenvalues form groups of (fine structure) multiplets, the total number of states per multiplet being equal to the dimensionality of the spin Hilbert space, 2^N. For clarity the lowest multiplets are magnified indicating the total spin of each level. The ground state energies are subtracted.

FIG. 9. Charge density $\varrho(x)$ for three electrons and various L, with normalization such that $\int \varrho(x)dx = 3$. When $L \gtrsim a_\mathrm{B}$, three peaks begin to emerge and become well separated for $L \gtrsim 100a_\mathrm{B}$.

FIG. 10. Potential landscape for two electrons in a 1D well, equivalent to the potential seen by a single (fictitious) equivalent particle in 2D.

FIG. 11. Classical configurations with minimum electrostatic energy for three electrons in a square dot. Quantum mechanically the system may be described approximately by a tight-binding model (t-model) in which the 'hole' hops between adjacent corners.

FIG. 12. Low-energy states of of interacting electrons in a square quantum dot. (a) 3 electrons given by solutions of the t-model, showing a spin-polarised ground state. (b) 4 electrons with singlet ground state from solution of the antiferromagnetic Heisenberg model. (c) 5 electrons with $S = 3/2$ ground state, again from the antiferromagnetic Heisenberg model.

FIG. 13. Low-energy classical configurations for two electrons in a square quantum dot which are described quantum mechanically by the tJV-model. The last four (higher energy) configurations may be eliminated by degenerate perturbation theory, resulting in a spin model which resonates between the two lowest-energy configurations.

FIG. 14. Electron configurations showing spin-blockade. Although the ground-state with four-electrons in a square dot plus an electron at the Fermi energy is degenerate with the ground-state with five electrons on the dot (so energy conservation would allow the current to flow), the transition is forbidden since the electron entering is not able to change the ground-state spin on the dot from $S = 0$ ($N = 4$) to $S = 3/2$ ($N = 5$). The same is true for the transition with one electron leaving the dot with five electrons.

FIG. 15. A six-step ring process for a triangular quantum dot, in which all three electrons rotate cyclically through $2\pi/3$.

FIG. 16. Gradual distortion of a triangular quantum dot into a circular dot during which the ground state switches from $S = 1/2$ (a) to $S = 3/2$ (c).
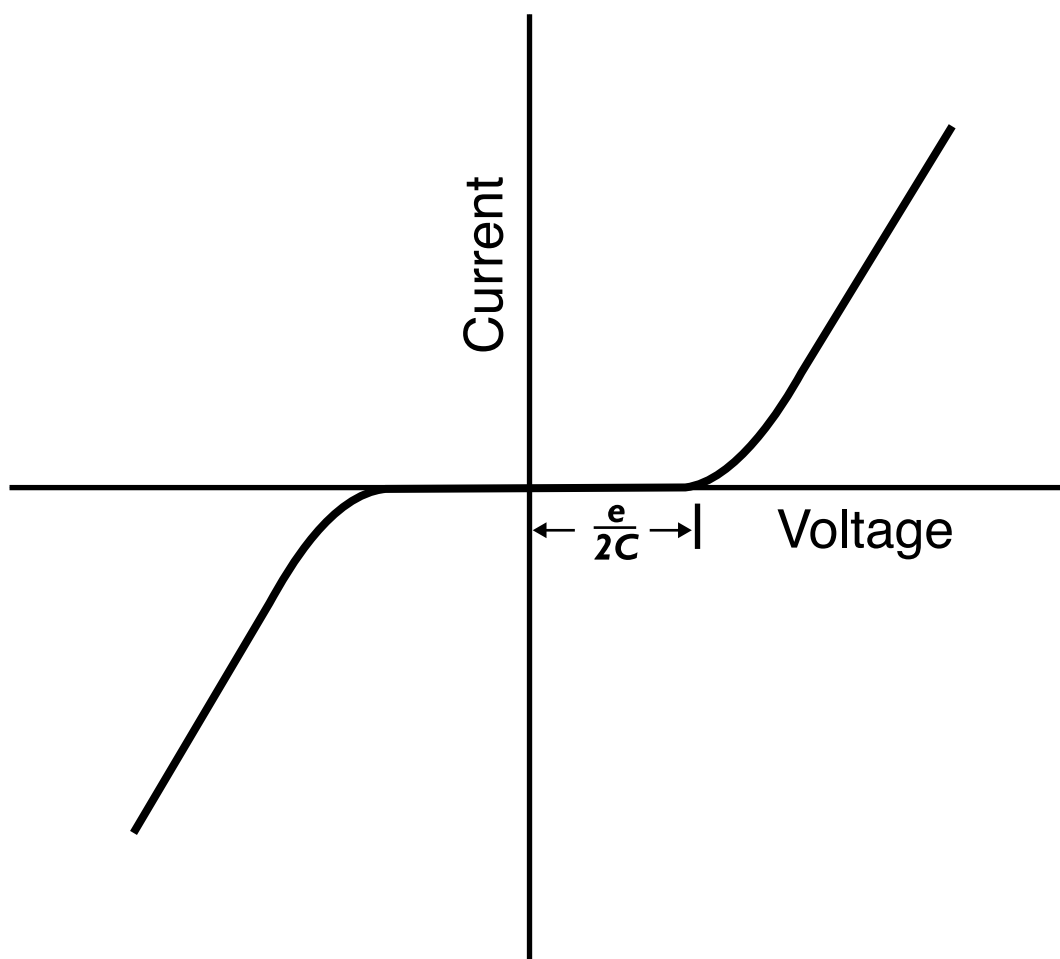
Current

Voltage

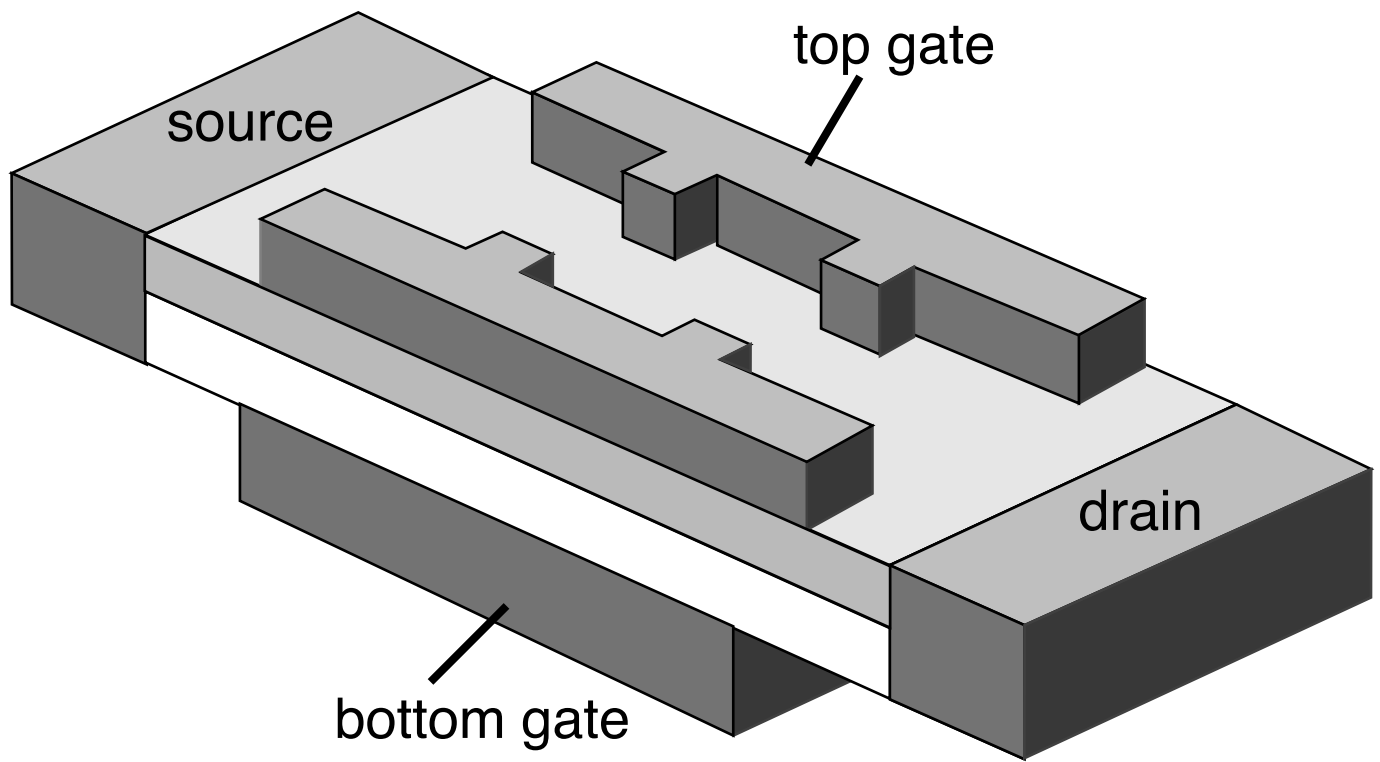$\frac{e}{2C}$

source

top gate

bottom gate

drain

FIGURE 2   JEFFERSON/HÄUSLER

21

source

dot

drain

FIGURE 3   JEFFERSON/HÄUSLER

Current

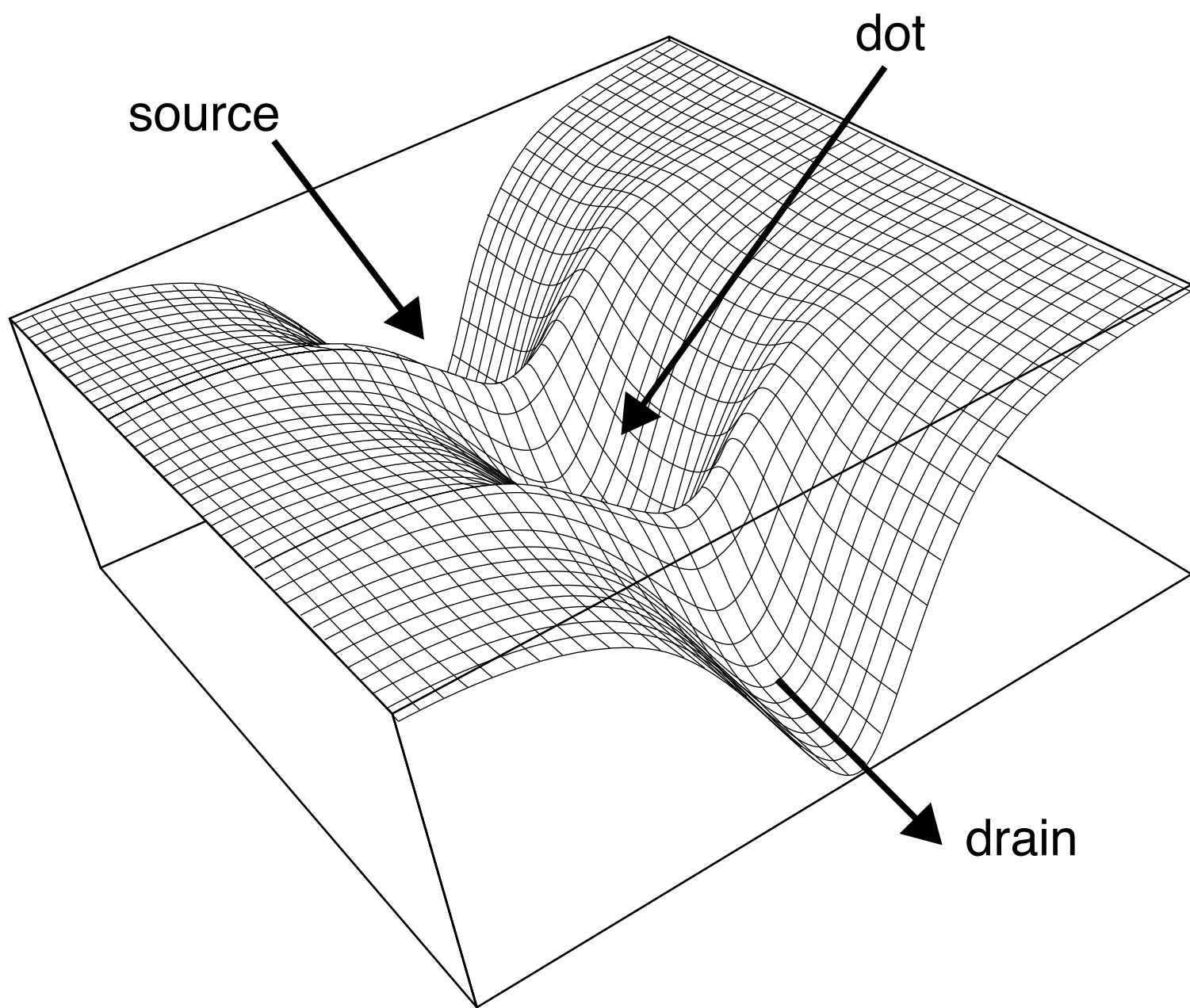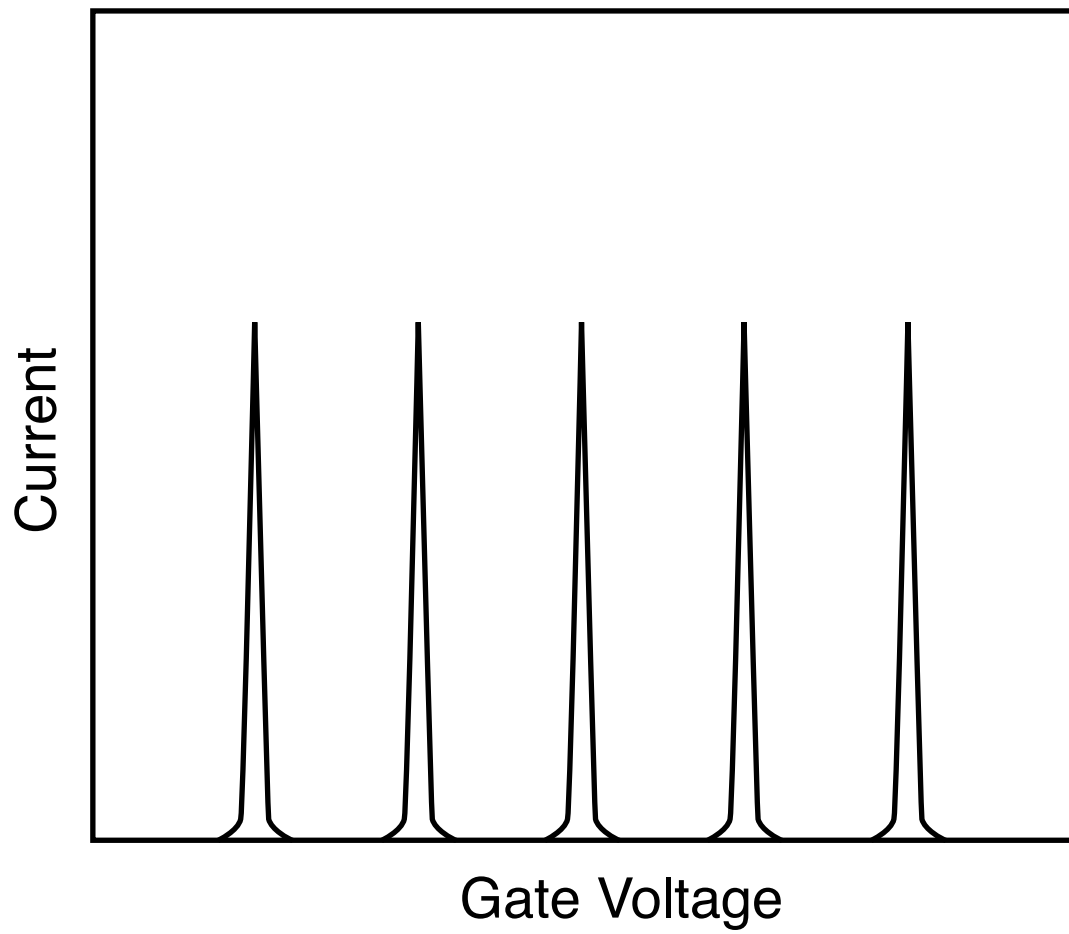Gate Voltage

FIGURE 4   JEFFERSON/HÄUSLER

23
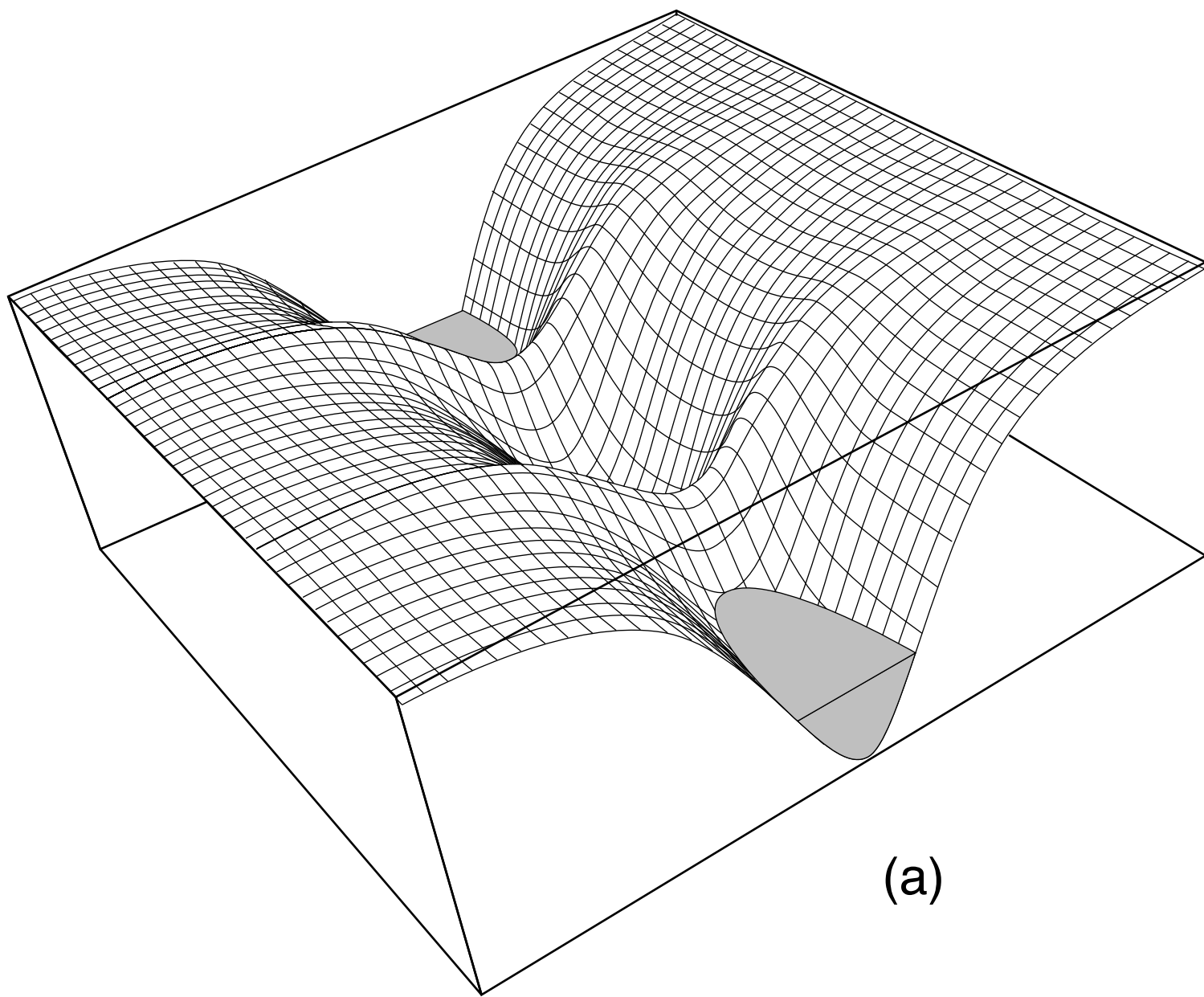
(a)

FIGURE 5a   JEFFERSON/HÄUSLER
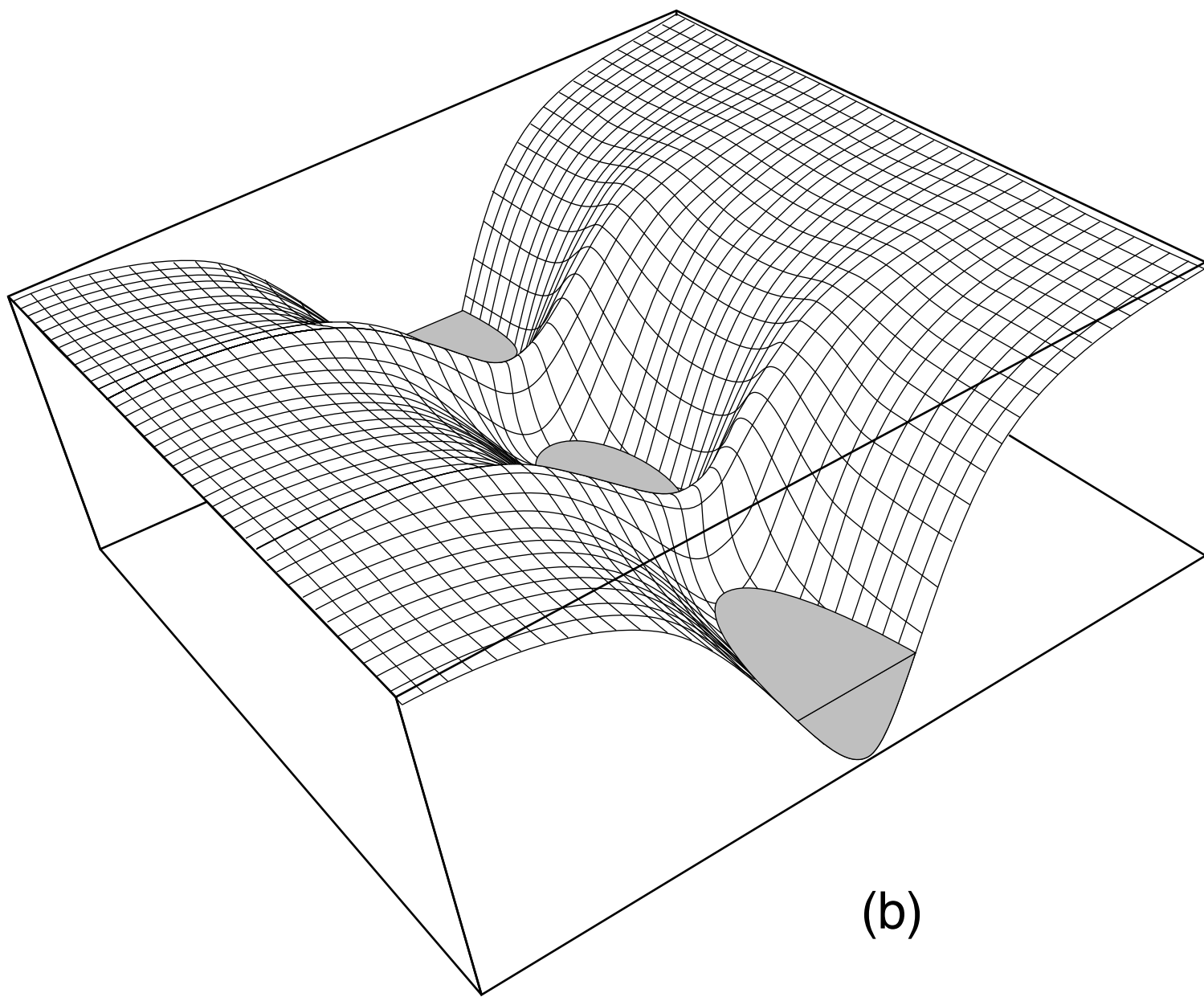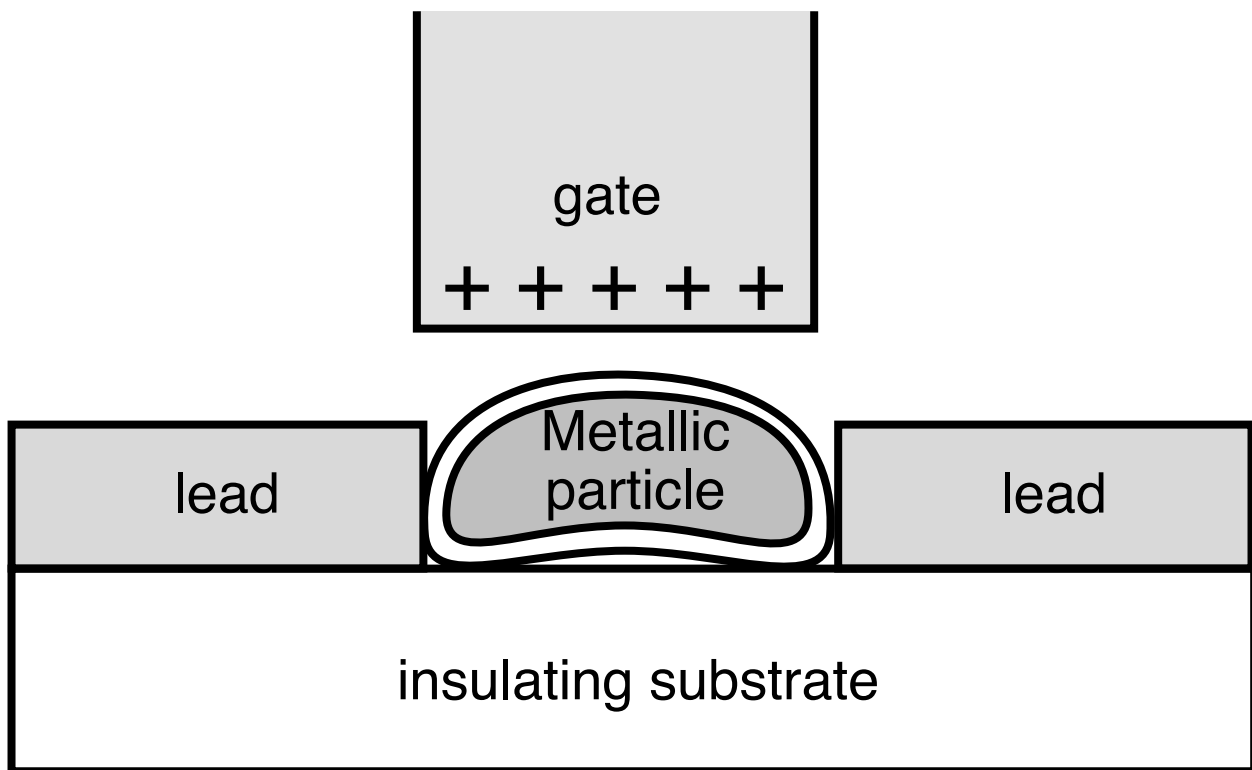
(b)

FIGURE 5b   JEFFERSON/HÄUSLER

gate

+ + + + +

Metallic particle

lead

lead

insulating substrate

FIGURE 6   JEFFERSON/HÄUSLER

26

(a)

(b)

(c)
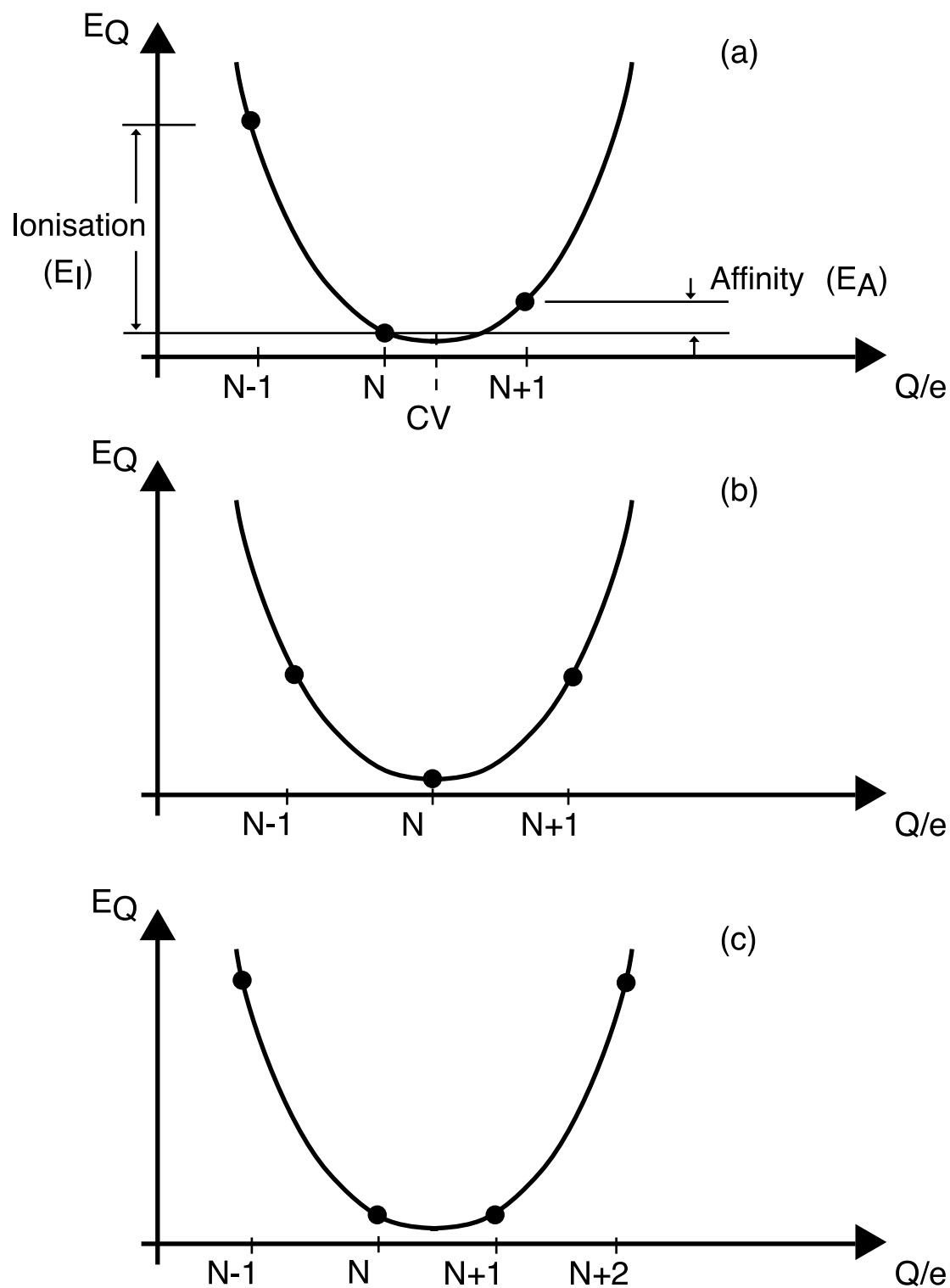
FIGURE 7   JEFFERSON/HÄUSLER

$$\frac{E_\nu - E_0}{E_H}$$
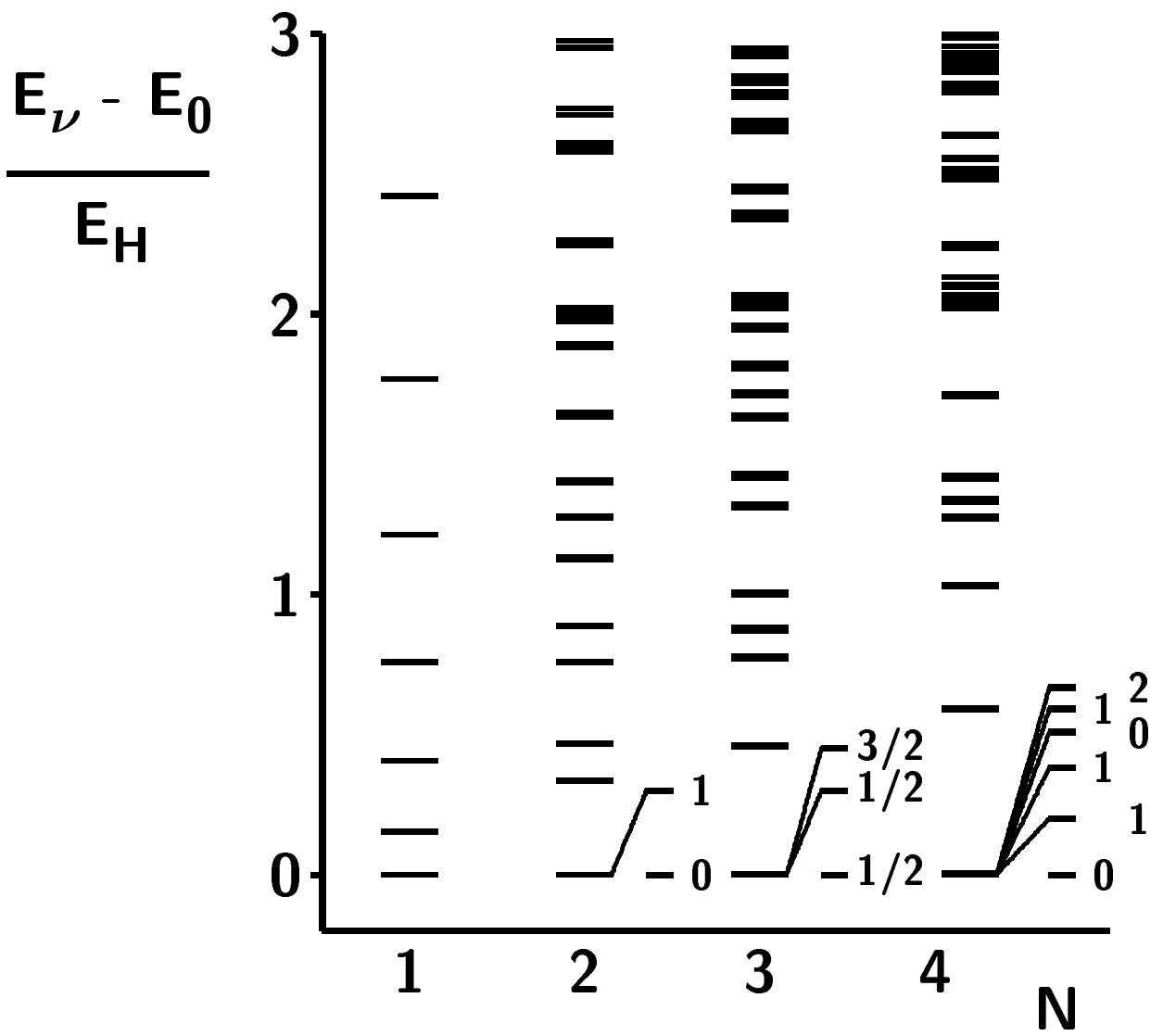
FIGURE 8   JEFFERSON/HÄUSLER
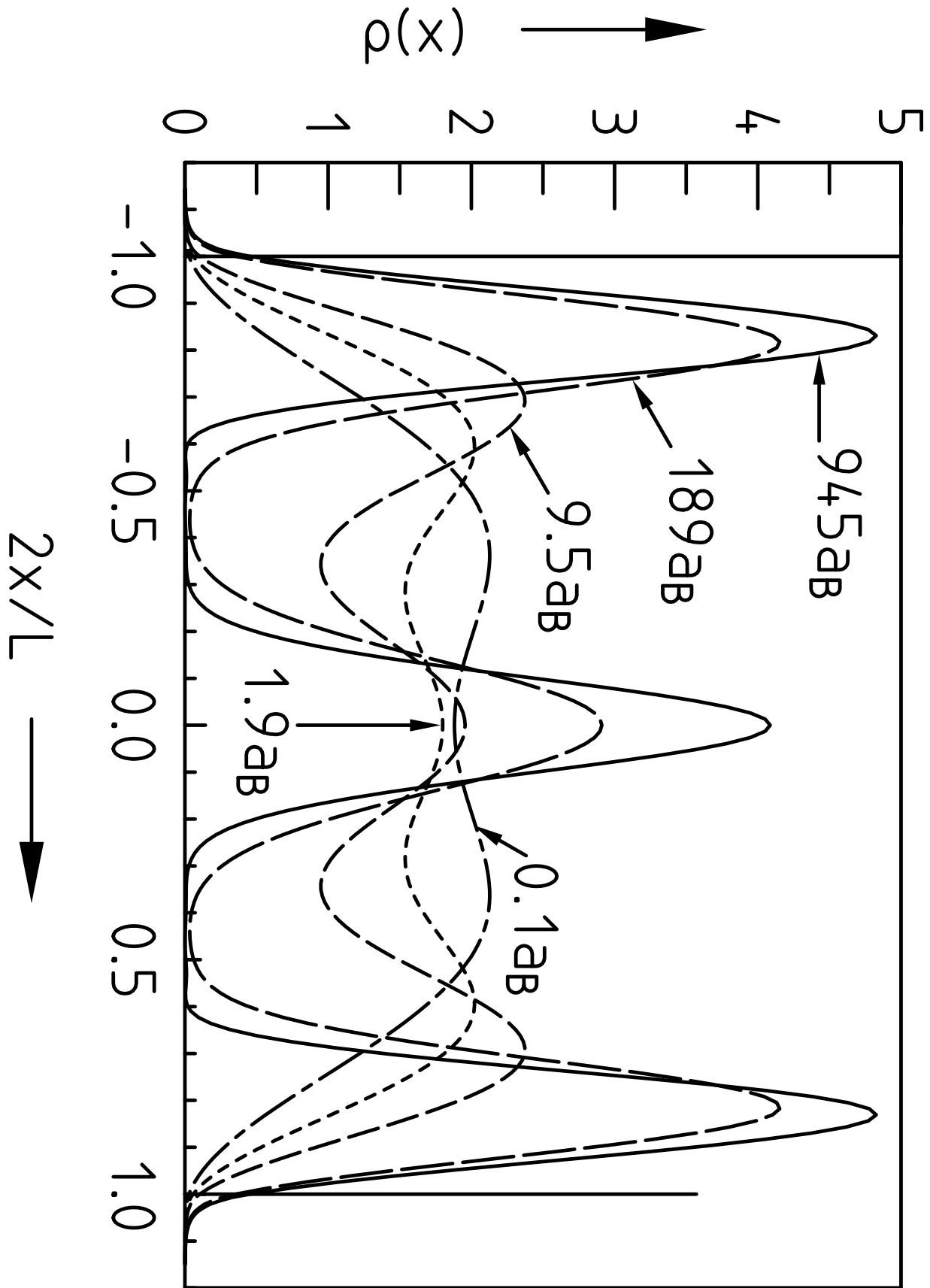
FIGURE 9   JEFFERSON/HÄUSLER

REGION 1

REGION 2
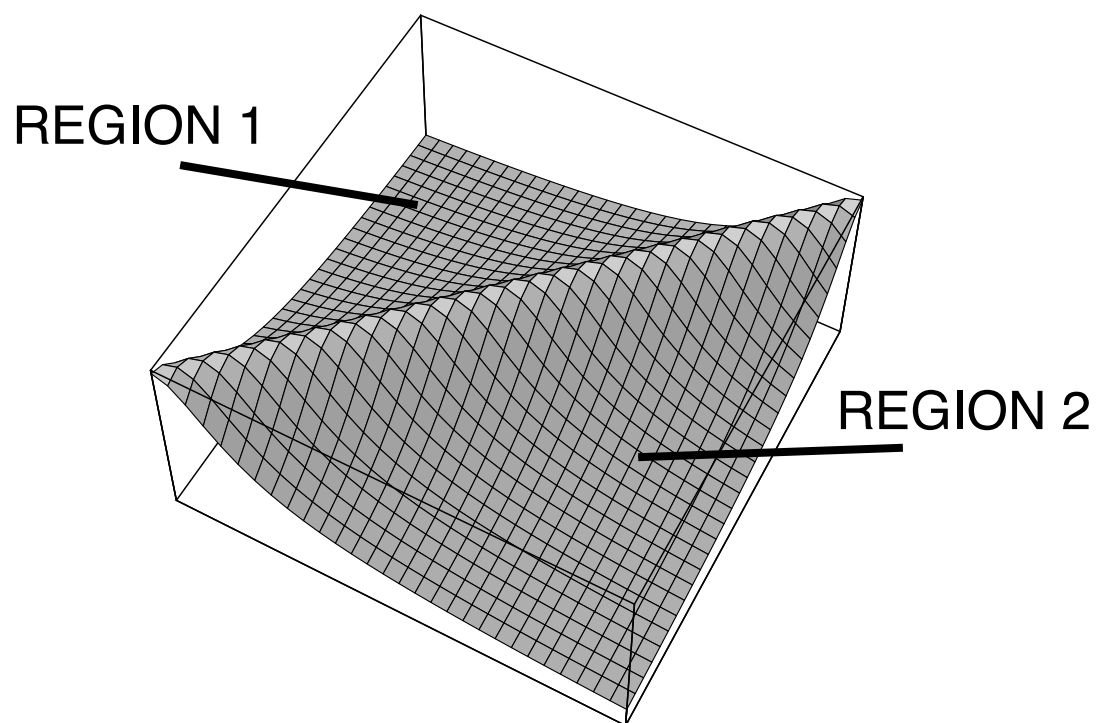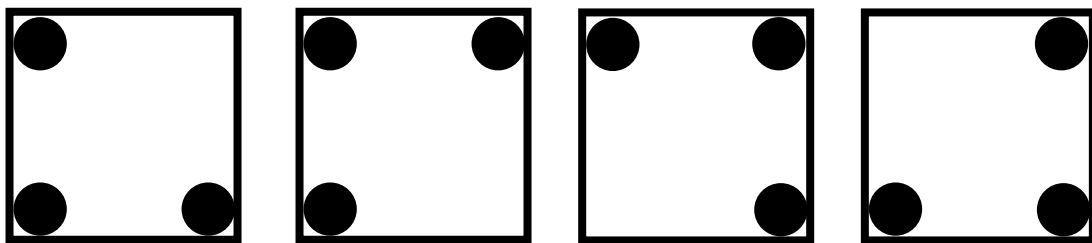
FIGURE 11   JEFFERSON/HÄUSLER

N = 3   **N = 4**   **N = 5**

4t — S = 3/2   3J — S = 2   5J/2 — S = 5/2
(2+√3)t — S = 1/2

                                     2J — S = 3/2,3/2,3/2

3t — S = 1/2,1/2

                   2J — S = 1,1,0   3J/2 — S = 1/2,1/2

2t — S = 3/2,3/2

                   J — S = 1

t — S = 1/2,1/2

                                     J/2 — S = 1/2,1/2,1/2

(2−√3)t — S = 1/2,1/2
0 — S = 3/2   0 — S = 0   0 — S = 3/2

(a)   **(b)**   **(c)**

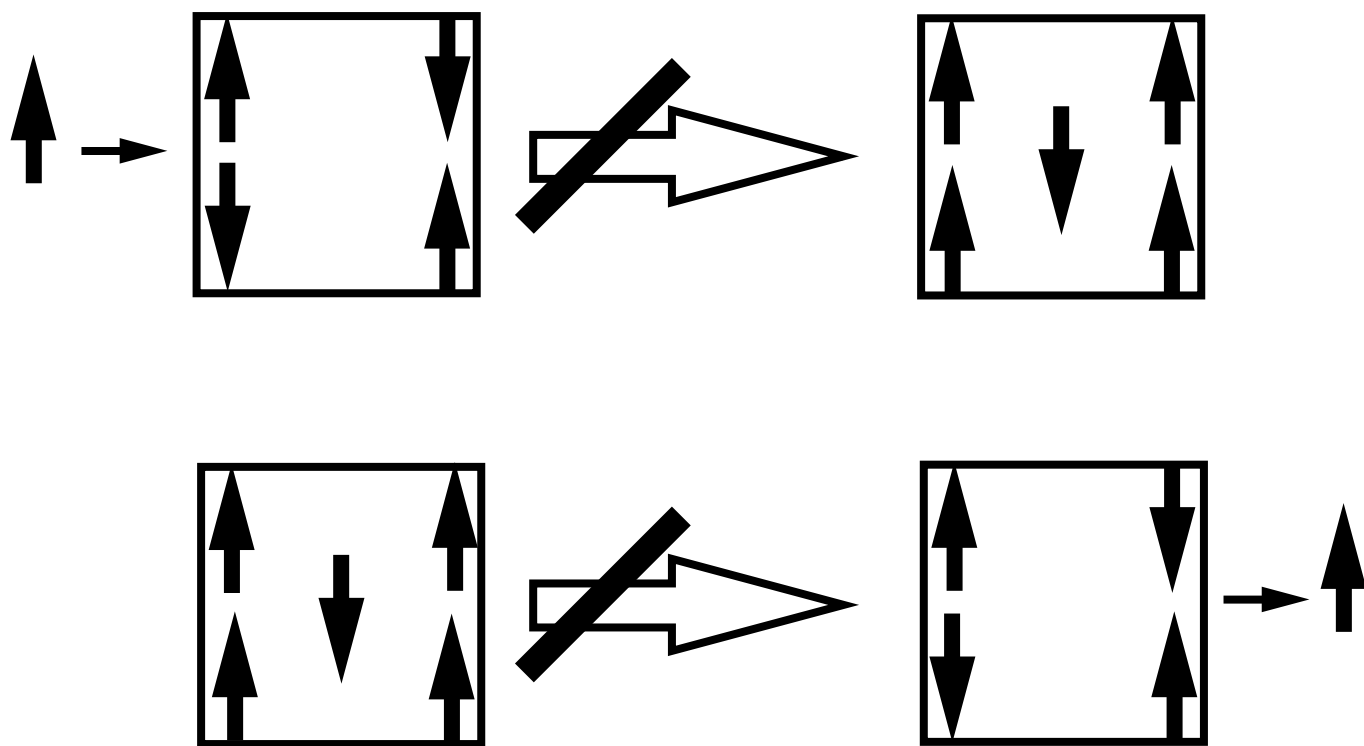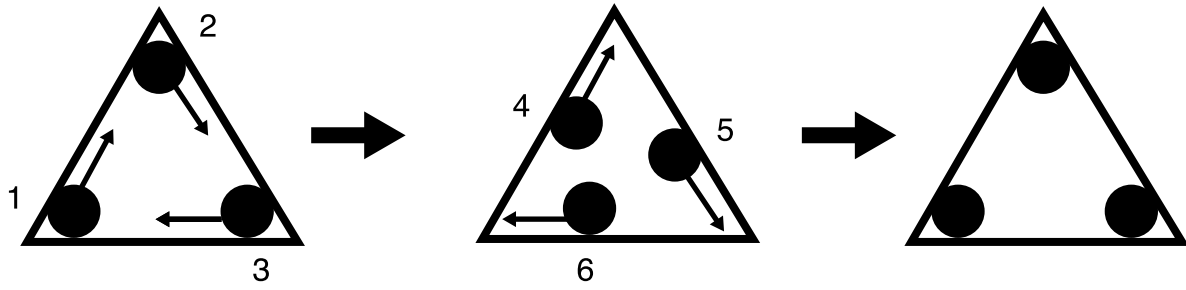FIGURE 12   JEFFERSON/HÄUSLER

32
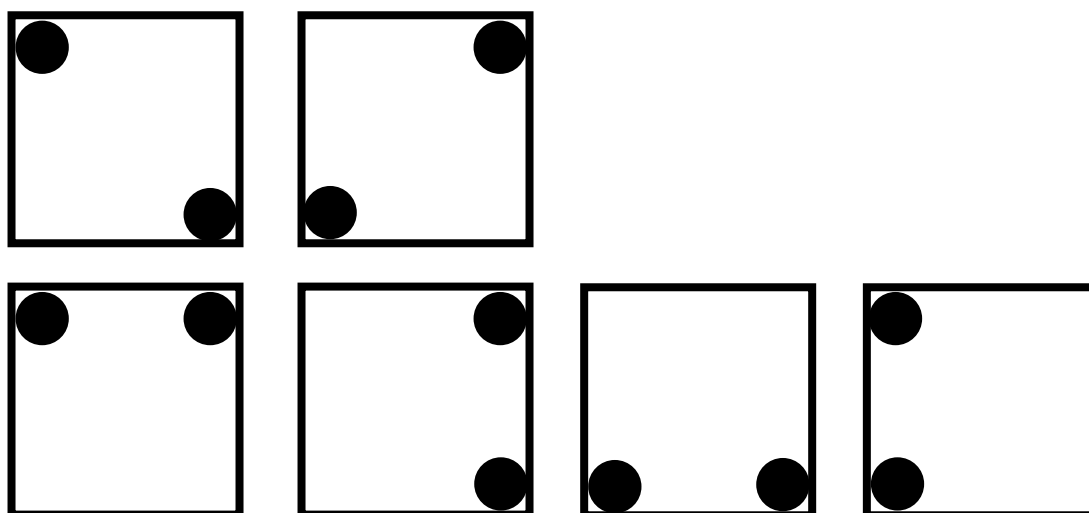
FIGURE 13   JEFFERSON/HÄUSLER
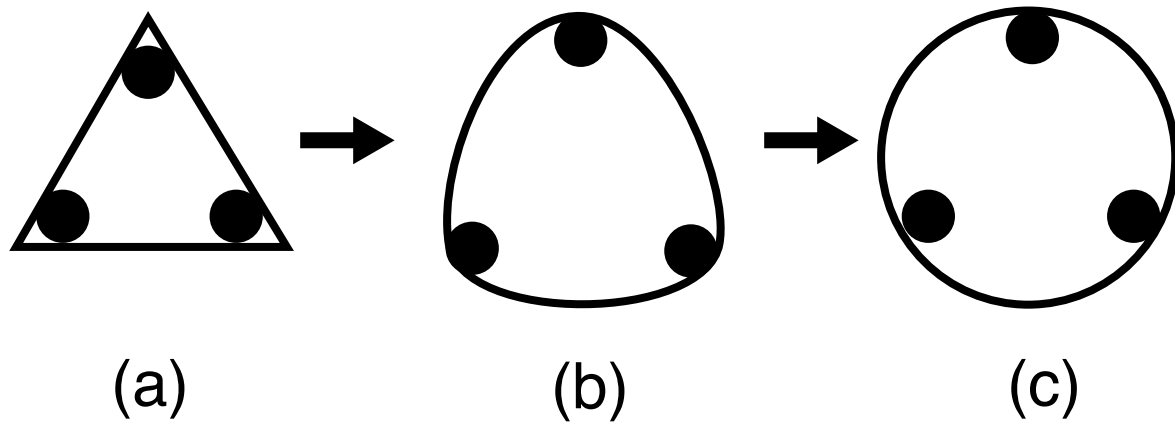
FIGURE 14   JEFFERSON/HÄUSLER

FIGURE 15   JEFFERSON/HÄUSLER

(a) → (b) → (c)

FIGURE 16   JEFFERSON/HÄUSLER

36